







Review

Hemodynamic Imaging in Cerebral Diffuse Glioma—Part B: Molecular Correlates, Treatment Effect Monitoring, Prognosis, and Future Directions

Vittorio Stumpo ^{1,2,*}, Lelio Guida ^{1,2,†}, Jacopo Bellomo ^{1,2}, Christiaan Hendrik Bas Van Niftrik ^{1,2}, Martina Sebök ^{1,2}, Moncef Berhouma ³, Andrea Bink ^{2,4}, Michael Weller ^{2,5}, Zsolt Kulcsar ^{2,4}, Luca Regli ^{1,2} and Jorn Fierstra ^{1,2}

- ¹ Department of Neurosurgery, University Hospital Zurich, 8091 Zurich, Switzerland; leliog06@gmail.com (L.G.); jacopo.bellomo@usz.ch (J.B.); bas.vanniftrik@usz.ch (C.H.B.V.N.); martina.seboek@usz.ch (M.S.); luca.regli@usz.ch (L.R.); jorn.fierstra@usz.ch (J.F.)
- ² Clinical Neuroscience Center, University Hospital Zurich, University of Zurich, 8057 Zurich, Switzerland; andrea.bink@usz.ch (A.B.); michael.weller@usz.ch (M.W.); zsolt.kulcsar@usz.ch (Z.K.)
- ³ Department of Neurosurgical Oncology and Vascular Neurosurgery, Pierre Wertheimer Neurological and Neurosurgical Hospital, Hospices Civils de Lyon, 69500 Lyon, France; moncef.berhouma@chu-lyon.fr
- ⁴ Department of Neuroradiology, University Hospital Zurich, 8091 Zurich, Switzerland
- ⁵ Department of Neurology, University Hospital Zurich, 8091 Zurich, Switzerland
- * Correspondence: vittorio.stumpo@usz.ch
- † These authors contributed equally to this work.



Citation: Stumpo, V.; Guida, L.; Bellomo, J.; Van Niftrik, C.H.B.; Sebök, M.; Berhouma, M.; Bink, A.; Weller, M.; Kulcsar, Z.; Regli, L.; et al. Hemodynamic Imaging in Cerebral Diffuse Glioma—Part B: Molecular Correlates, Treatment Effect Monitoring, Prognosis, and Future Directions. *Cancers* **2022**, *14*, 1342. <https://doi.org/10.3390/cancers14051342>

Academic Editor: Shinji Kawabata

Received: 1 February 2022

Accepted: 2 March 2022

Published: 5 March 2022

Publisher's Note: MDPI stays neutral with regard to jurisdictional claims in published maps and institutional affiliations.



Copyright: © 2022 by the authors. Licensee MDPI, Basel, Switzerland. This article is an open access article distributed under the terms and conditions of the Creative Commons Attribution (CC BY) license (<https://creativecommons.org/licenses/by/4.0/>).

Simple Summary: Cerebral diffuse gliomas present peculiar molecular features tightly linked to phenotypic characteristics that are not readily appreciated by means of standard neuroimaging. In the present Part B of our two-review series, the potential of exploiting glioma vascular and hemodynamic alterations for a better characterization of tumor subtype, differentiation of tumor recurrence from treatment effects, and prognosis prediction is critically discussed together with the advancements related to radiomics and machine learning for innovative imaging biomarkers development.

Abstract: Gliomas, and glioblastoma in particular, exhibit an extensive intra- and inter-tumoral molecular heterogeneity which represents complex biological features correlating to the efficacy of treatment response and survival. From a neuroimaging point of view, these specific molecular and histopathological features may be used to yield imaging biomarkers as surrogates for distinct tumor genotypes and phenotypes. The development of comprehensive glioma imaging markers has potential for improved glioma characterization that would assist in the clinical work-up of preoperative treatment planning and treatment effect monitoring. In particular, the differentiation of tumor recurrence or true progression from pseudoprogression, pseudoresponse, and radiation-induced necrosis can still not reliably be made through standard neuroimaging only. Given the abundant vascular and hemodynamic alterations present in diffuse glioma, advanced hemodynamic imaging approaches constitute an attractive area of clinical imaging development. In this context, the inclusion of objective measurable glioma imaging features may have the potential to enhance the individualized care of diffuse glioma patients, better informing of standard-of-care treatment efficacy and of novel therapies, such as the immunotherapies that are currently increasingly investigated. In Part B of this two-review series, we assess the available evidence pertaining to hemodynamic imaging for molecular feature prediction, in particular focusing on isocitrate dehydrogenase (IDH) mutation status, MGMT promoter methylation, 1p19q codeletion, and EGFR alterations. The results for the differentiation of tumor progression/recurrence from treatment effects have also been the focus of active research and are presented together with the prognostic correlations identified by advanced hemodynamic imaging studies. Finally, the state-of-the-art concepts and advancements of hemodynamic imaging modalities are reviewed together with the advantages derived from the implementation of radiomics and machine learning analyses pipelines.

Keywords: hemodynamic; diffuse glioma; glioblastoma; molecular features; perfusion MRI; cerebrovascular reactivity; tumor progression; radiation necrosis; prognosis; radiomics; machine learning

1. Introduction

In recent decades, the traditional histopathological grading of diffuse gliomas has been complemented by a more refined molecular analysis of tumor markers. Gliomas, and glioblastomas in particular, exhibit an extensive intra- and inter-tumoral molecular heterogeneity which represent complex biological features, correlating to the efficacy of treatment response and survival [1]. This broadened understanding has translated into a more comprehensive WHO classification of high grade gliomas [2] as well as more tailored treatment guidelines [3]. Importantly, from a neuroimaging point of view, these specific molecular and histopathological features may be used to yield imaging biomarkers as surrogates for distinct tumor genotypes and phenotypes [4]. The development of comprehensive glioma imaging markers has potential for improved glioma characterization that will assist in the clinical work-up of preoperative treatment planning and treatment effect monitoring. Current imaging techniques are yet to overcome certain limitations which, until now, have prohibited a clear demarcation of the diffuse glioma infiltration zone as well as the molecular phenotypes present within the lesion. These aspects are of particular clinical relevance since the differentiation of tumor recurrence or true progression from pseudoprogression, pseudoresponse, and radiation-induced necrosis are still not reliably determined through standard neuroimaging only [5]. Given the abundant vascular and hemodynamic alterations present in diffuse glioma, advanced hemodynamic imaging approaches constitute an attractive area of clinical imaging development (Figure 1).

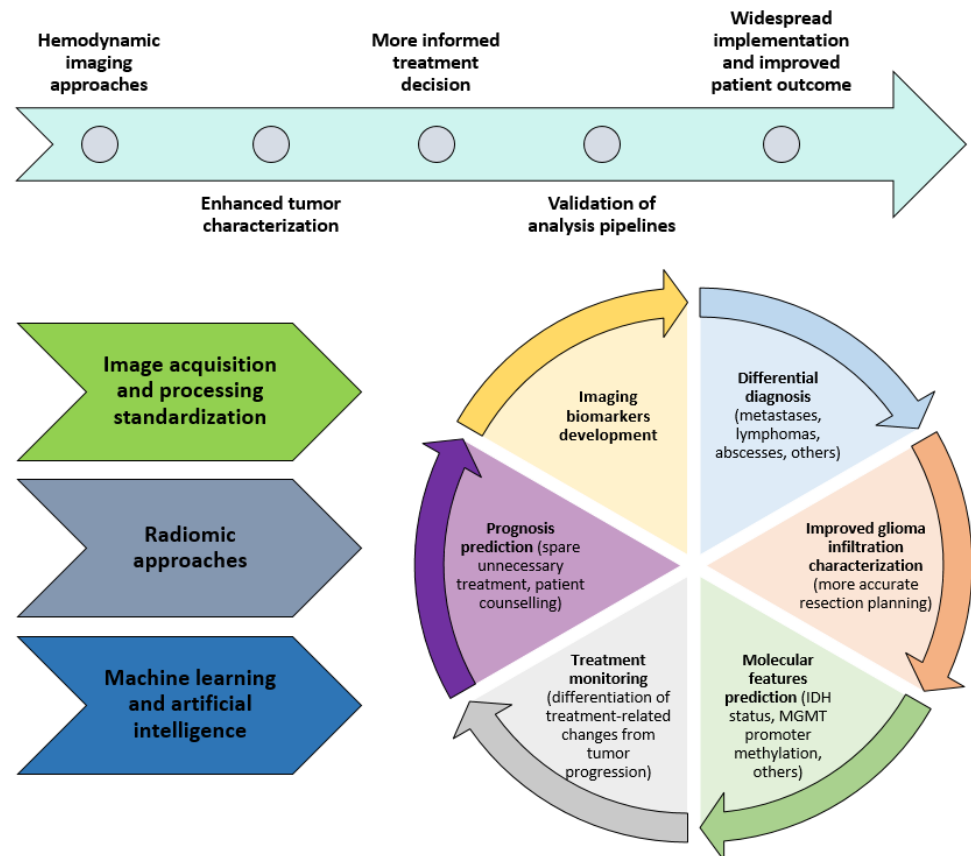


Figure 1. Schematic representing the overview of hemodynamic imaging past progress and future potential for enhanced glioma characterization.

Hemodynamic imaging of brain tumors adopts several techniques, including perfusion MRI sequences, such as dynamic susceptibility contrast (DSC)-MRI, dynamic contrast-enhanced (DCE)-MRI, arterial spin labelling (ASL)-MRI and perfusion computed tomography (PCT) together with a number of other advanced hemodynamic imaging approaches that are increasingly investigated. A description of hemodynamic imaging modalities and relative assessed parameters is presented in Part A of the present review (see Tables 1 and 2 of Part A) [6].

In this context, the inclusion of objective measurable glioma imaging features may have the potential to enhance the individualized care of diffuse glioma patients, which can better inform standard-of-care treatment efficacy and novel therapies, such as immunotherapies that are currently being increasingly investigated [7]. In Part B of this review, we assess the available evidence pertaining to hemodynamic imaging for molecular feature prediction. The results on the differentiation of tumor progression/recurrence due to treatment effects have also been the focus of active research and are presented together with the prognostic correlations identified by advanced hemodynamic imaging studies. Finally, state-of-the-art concepts and advancements in hemodynamic imaging modalities are reviewed together with the advantages derived by the implementation of radiomics and the machine learning analyses pipelines.

2. Clinical Applications of Hemodynamic Imaging in Gliomas—Part 2

2.1. Molecular Features Prediction

With the increasingly understood role of biology in correlating tumor aggressiveness and prognosis, the old histological entities are now outdated and tumor classification depends on underlying molecular features [2]. This information, which is crucial in patient management, is currently only available after the analysis of tumor specimens (biopsy/resection). In this respect, advancements in neuroimaging can play a determinant role in inferring the tumor characteristics, metabolism, and micro-structure [8] but they also provide additional means of correlating the imaging biomarkers to the tumor molecular features pre-operatively, i.e., radiogenomics [9]. Examples of efforts in this direction include the availability of the Cancer Genome Atlas imaging datasets through the Cancer Imaging Archive (<https://www.cancerimagingarchive.net/> Last accessed on 21 December 2021). More importantly, this hypothesis has been also extensively explored in hemodynamic imaging [10–35]. In this section, we focus in particular on hemodynamic correlates of isocitrate dehydrogenase (IDH) mutation status, 1p19q codeletion, O⁶-methylguanine-DNA methyl-transferase (MGMT) promoter methylation, and epidermal growth factor receptor (EGFR) alterations.

2.2. IDH Mutation Status

IDH mutations are the most important prognostic factors according to the present molecular classification of gliomas whereby the absence of mutation (mut), i.e., IDH wild-type (wt) tumors, is characterized by a worse prognosis. IDH1/2 mutations occurring in the catalytic pocket generate a neomorphic enzyme that converts α -ketoglutarate and NADPH to (R)-2hydroxyglutarate (2-HG). The IDHmut and the accumulation of the “oncometabolite” 2-HG are associated with the hypermethylation phenotype, called glioma CpG island methylator, ultimately altering metabolism to promote malignant growth [36,37]. As the prognostic implications of reliable pre-operative identification of this molecular marker could significantly alter the clinical management decisions including the radicality of the surgical resection, several studies have investigated the potential for IDH status prediction in diffuse gliomas using hemodynamic imaging [10,11,20,29,30,32,38]. Consistently with “traditional” tumor grading, IDHmut gliomas tend to exhibit decreased perfusion and permeability with respect of their wild-type counterpart. Lower DSC-cerebral blood volume (CBV) [10,20,29,32,39,40], as with lower DSC-cerebral blood flow (CBF) [30,38], were found to be able to discriminate IDHmut versus IDHwt. Percentage of signal recovery (PSR) was also reported to be lower in IDHwt tumors [40]. DCE studies assessing the per-

meability parameters also showed potential for distinguishing between the two molecular entities. IDHmut gliomas were found to exhibit decreased CBF, volume transfer constant between blood plasma and extravascular extracellular space (K_{trans}), blood plasma fractional volume (V_p), extravascular extracellular volume fraction (V_e), and area under the curve (AUC) [11,41,42]. With respect of ASL-CBF, some authors like Brendle et al. and Yoo et al. reported it to be useful to distinguish between these two subgroups [43,44], while others found only a moderate correlation [12]. Consistently with these findings, PCT studies have also described decreased CBV and permeability surface area product (PS) in IDHmut gliomas [45]. These hemodynamic findings altogether support the concept of IDHmut tumoral tissue with reduced microvascular density and permeability with respect of IDHwt. This is consistent with their decreased aggressiveness and reduced activation of the hypoxic-angiogenic pathway [29,46].

2.3. *p/19q Codeletion*

Oligodendroglioma is genetically defined as a tumor harboring a IDH1/IDH2 mutation involving the co-deletion of chromosome arms 1p and 19q. Diagnosis can be obtained only using pathological tissue after a biopsy or resection [3,47] but hemodynamic imaging has also shown potential for the identification of IDH 1p/19q codeletion status as part of the differentiation of oligodendroglioma from the IDH mutant 1p/19q non-deleted astrocytomas and IDHwt glioblastomas [10–12,30,48]. The pre-operative identification of 1p/19q is clinically relevant as oligodendrogliomas are characterized by a lower impact of the extent of resection with respect of IDHmut astrocytoma, whereas they also display a better response to cytotoxic agents and increased OS [49]. DSC-CBV has been found to be increased in IDHmut 1p/19q codeletion grade 3 gliomas as opposed to IDHmut 1p/19q non-codeletion grade 3, [30,48,50,51] suggesting denser and more heterogeneous vascular distribution in the former [48], but decreased with respect to IDHwt glioblastomas [10,50,52]. In a meta-analysis by Delgado and Delgado investigating whether DSC can differentiate between grade 2 and 3 gliomas, diagnostic accuracy was substantially decreased for differentiating between oligodendroglioma grades 2 and 3 [53]. With respect of DCE, Conte et al. found that there were no difference in DCE parameters when distinguishing between IDHmut gliomas with or without 1p/19qdel [11] in line with the findings of Yoon et al. [52]. These instead reported K_{trans} and V_e to be significantly decreased in grade 2–3 oligodendrogliomas compared with glioblastomas [52]. On the contrary, a study by Lee et al. using histogram analysis reported increased K_{trans} , V_e in grade 2–3 oligodendrogliomas versus astrocytomas grade 2–3 [51]. ASL-derived CBF used to predict IDH genotype and 1p/19q codeletion, despite showing a moderate correlation in some studies, failed to reach a significant association in others [12,44]. PCT studies reported a higher CBV and lower PS in 1p/19q codeletion gliomas compared with the intact counterparts [54].

2.4. *MGMT Promoter Methylation*

MGMT promoter methylation has drawn considerable attention as its presence contributes to the response to temozolomide. A selected population of MGMT unmethylated glioblastoma patients may reach a comparable outcome when chemotherapy is withheld [55]. Due to its potential to drive management decisions, a number of studies have investigated the possibility to pre-operatively identify MGMT promoter methylation through hemodynamic imaging [31,34,35,56,57] despite some investigations having reported histopathological and immunohistochemical analysis not differing significantly between these two phenotypes [58]. In line with the concept so far explored, indicating that increased tumor perfusion correlates to aggressiveness, MGMT methylated gliomas have also been found to exhibit decreased CBV [59–61] as well as decreased peak height (PH) [59]. CBF differences were not found in DSC studies [60]. Nevertheless, the evidence is conflicting as a previous smaller series by Moon et al. observed no significant difference in CBV [56]. The results were also confirmed in a larger study population described by Fuster-Garcia et al. [62]. Interestingly, a recent study by Choi et al. showed that DSC-CBV

in a non-enhancing tumor could be used to predict methylation status change at recurrence [35]. Similar conflicting evidence has been reported in DCE studies. Zhang et al. utilized DCE-parameters in a histogram analysis and found increased V_e and K_{trans} in MGMT unmethylated tumors [40]. These findings contradict a previous study by Ahn et al. who on the contrary reported reduced K_{trans} in MGMT unmethylated tumors [31]. Further complicating the matter, one study reported that ASL-CBF in CE was found to be significantly higher in unmethylated versus methylated gliomas [43].

2.5. EGFR Mutation

Following the detection of epidermal growth factor receptor (EGFR) gene alterations (such as amplifications, mutations, and translocation) in a high percentage of glioblastomas, the attempt to develop treatment strategies targeting EGFR has been pursued [63]. Given the availability of receptor-tyrosine kinase inhibitors and the possibility of testing these drugs in clinical trials (with at present disappointing results [64]), the non-invasive imaging of EGFR alteration is clinically relevant and hemodynamic imaging approaches have been attempted [26,33,65–67]. DSC-CBV was reported to be significantly higher in EGFRvIII expressing tumors than in wild-type ones [67]. Gupta et al. reported a higher CBV (finding not confirmed by Oughourlian et al. [68]) and lower PSR in tumors with EGFR amplification, while EGFRvIII mutated tumors were associated with higher PH [65]. DCE studies found higher V_p and K_{trans} , with the former histogram metrics outperforming the latter for this aim [66]. A study by Qiao et al. found there to be a significant association between a ASL-CBF hypervascular pattern identified with high inter-rater agreement and EGFRvIII expression [33].

2.6. Other Markers: Hypoxia, Angiogenesis, Proliferation

Given the relationship of aberrant glioblastoma vasculature with hypoxia playing a role in its development and invasion, a number of studies have investigated the potential for correlating the perfusion measures to hypoxic and angiogenic markers [16,18,21,23–28,69,70]. In parallel, markers of cellular proliferation—indicating tumor malignancy—such as Ki67 have been correlated to perfusion parameters [14,15,28]. The genetic heterogeneity characteristic of diffuse cerebral glioma results in deregulated molecular pathways whose more relevant effectors such as TERT, ATRX, PTEN, and mTOR have also been correlated to perfusion imaging [40,59,71].

2.7. Differentiation between Tumor Progression/Tumor Recurrence vs Radiation Necrosis/Pseudoprogression/Pseudoresponse

An additional clinically relevant limitation of the current standard imaging is a suboptimal differentiation between tumor progression/recurrence and radionecrosis, pseudoprogression, or pseudoresponse [72]. Pseudoprogression, with a reported variable incidence rate of 10 to 30% in patients receiving chemoradiotherapy, is defined by the presence of new or enlarging area(s) of contrast-enhancement in the absence of true tumor growth which regresses or stabilizes despite no changes in treatment [73]. Due to its similarities with the other above-mentioned entities, diagnosis is usually retrospective but it can be also obtained by the tissue sample analysis. Pathophysiologically, this phenomenon is likely to be determined by the transiently increased capillary permeability of pathological vasculature as well as by the inflammation determined through chemoradiotherapy. The difference to radiation necrosis is related both to the timing of presentation, i.e., 3–6 months for pseudoprogression and 1 year after radiation therapy in radiation necrosis, but also to the different pathophysiology whereby radiation necrosis presents as permanent damage to the brain tissue, necrosis, and vascular thrombosis [74]. Variable “timing” definitions and the blurred presentation between these two entities reported in published studies have important implications in terms of patient management, clinical trial enrolment, and treatment evaluation [75]. In fact, patients with pseudoprogression are notably characterized by a favorable clinical course. On the opposite spectrum, falsely favorable imaging signs

are present in pseudoresponse whereby the use of antiangiogenic treatment, i.e., VEGF inhibitors induce the normalization of the BBB, thus leading to a reduction in contrast enhancement and edema in the T2/FLAIR sequence. In this case, the observed improvement is a sole consequence of the alterations in vascular permeability and is thus unrelated to treatment efficacy [5]. Some other chemotherapeutic treatments can also induce imaging abnormalities and an accurate distinction from relapse is therefore needed [76]. Several studies have addressed this clinical issue [76–99]. As for the other previously presented outcomes, DSC has been more extensively investigated. A number of research groups confirmed DSC-CBV to be higher in tumor recurrence/progression versus radiation necrosis [78,79,81–83,89,91,93,94,97,100–103]. These results have been accordingly strengthened by meta-analyses [104–107]. Chuang et al. in 2016 performed a random effect model meta-analysis of ten studies evaluating CBV and found that this parameter is increased in the contrast-enhancing lesion of tumor recurrence versus radiation injury [105]. Another meta-analysis by Patel et al. found that after selecting the best performing parameter from each study, the pooled sensitivity and specificity were 0.90 and 0.88 respectively [106]. Wang et al. meta-analyzed 20 studies that adopted DSC and found that the pooled sensitivity and specificity were 0.83 and 0.83 respectively, while the AUC was 0.89 [104]. A more recent study by Tsakiris evaluating the differentiation of true tumor progression versus pseudoprogression using a random effect model in five DSC studies found there to be a pooled sensitivity and specificity of 0.81 and 0.82 [107]. Some studies also found that certain histographic patterns are the best independent predictors of tumor recurrence [87]. CBV is also lower in bevacizumab-induced abnormalities than in recurrent tumors [76]. A few publications also investigated other DSC parameters. For example, PH and PSR were found to be respectively increased and decreased in tumor recurrence [93].

DCE was more scarcely assessed but provided analogous results [82,88,95,96]. Ktrans has been found to be consistently higher in tumor progression/recurrence as opposed to radiation necrosis [82,88,95]. The same pattern was observed for iAUC [82,88]. A more detailed AUC analysis methodology was also applied by Suh et al. who could, with high sensitivity and specificity, differentiate between the two entities [99]. Vp and Ve were reported to be higher in progressive lesions versus radiation necrosis and pseudoprogression [95,96], while other reports found there to be no significant difference [88]. Pooled sensitivity and specificity were confirmed through a series of meta-analyses. Tsakiris et al. also evaluated performance in a random effect meta-analysis of DCE in the differential diagnosis between tumor progression and pseudoprogression. They found there to be a pooled sensitivity and specificity of 0.88 and 0.77, respectively [107]. In their meta-analysis including four DCE studies, Wang et al. found a pooled sensitivity and specificity of 0.73 and 0.80, and an AUC of 0.94 [104]. Okuchi et al. meta-analyzed nine studies for a total of 179 TR and 119 treatment-related changes. They found there to be a pooled sensitivity and specificity of 0.88 and 0.86, respectively, and an AUC of 0.89 [108]. ASL has been less investigated. Despite Myoshi et al. finding no correlation with tumor recurrence [109], another study by Nyberg et al. showed ASL-CBF to be more sensitive than standard imaging for identifying tumor progression in patients treated for high-grade glioma [110]. In the three studies assessing ASL included in Wang's meta-analysis, the pooled sensitivity and specificity were 0.79 and 0.78, respectively, and the AUC was 0.89 [104]. PCT studies on a few patients have also shown that CBV and CBF are increased in tumor recurrence, while mean transit time (MTT) is decreased [111,112]. The PS was also significantly decreased regarding the treatment-induced changes [111].

2.8. Prognosis Prediction

In the treatment of diffuse cerebral glioma, a precise stratification of outcome can support the multidisciplinary team caring for the patient, strengthening the evidence-based therapeutic decisions. Currently, a prognostic evaluation is based on clinical factors, standard imaging, and histopathological-immunochemical tissue analysis [3]. Ultimately, hemodynamic imaging-based differential diagnosis, the prediction of grading, molec-

ular features, and the differentiation of recurrent disease from the treatment effects, if proven with strong evidence, will all have a prognostic correlation. Before any inferences about prognosis can be drawn, the identification of an association requires sound methodology [113]. In this section, the associations of hemodynamic imaging-derived parameters to prognostic outcome prediction, such as a response to treatment, progression free survival (PFS) [24,33,50,114–121], and overall survival (OS) [20,23,24,122–124] are reviewed. As a general rule, pre-treatment increased tumor vascularity and BBB leakage (and related perfusion and permeability parameters) correlate with tumor malignancy and invasiveness. As a result, they are correlated with a worse prognosis while response to chemoradiotherapy has been associated with a decrease in tumor perfusion and BBB permeability. Increased DSC-CBV was found to be predictive of decreased progression free survival [20,116–119,125–127] and decreased OS [20,71,117,119,122–125,128–130,130–134] in diffuse cerebral gliomas. These parameters can be also used to follow-up on lower grade glioma lesions and to monitor treatment effects [122,135,136]. An increase in DSC-CBV during follow up of low-grade gliomas has, for example, been suggested to predict malignant transformation [137]. Moreover, an increase in CBV after chemoradiotherapy was also found to be a predictor for decreased OS [102]. In accordance with this, the clinical trials on recurrent glioblastoma prospectively evaluating perfusion MRI found that a decrease in CBV after treatment correlated to increased OS and increased CBV with respect to the baseline was instead associated with decreased OS [138]. In another trial, low CBV pre-treatment was predictive of an early response to bevacizumab and improved OS [139]. DSC-CBF has also shown a trend of significance for predicting time to recurrence but has been less commonly investigated. With respect of the DCE studies, increased Ktrans was shown to be associated with decreased PFS [140–143] and OS [125,143–146] in several studies. Of specific interest, the baseline elevated Ktrans in non-enhancing T2 lesions has been independently associated with negative PFS [141]. In accordance, a study by Kickingereder et al. in 2015 reported that recurrent GBM patients with lower baseline Ktrans and higher voxel wise reductions were characterized by increased PFS and OS [147]. Similarly to DSC derived measures, DCE-derived Ktrans is found to decrease significantly after chemoradiotherapy [148,149] and anti-angiogenic treatment [139,150], and to correlate with OS [148]. A high post-treatment Ktrans, accordingly, predicts decreased PFS [142]. Møller et al. used DCE to assess the CBF changes during chemoradiotherapy. They reported that it increased early on in the treatment only to decrease to a level lower than the baseline after the treatment ended. Neither of these changes nor the baseline values were determined to be correlated to PFS [151]. Lower Kep was found associated with a favorable response to bevacizumab in recurrent high-grade glioma, and increased Kep was on the contrary associated with shorter PFS and OS [114,152], even if these observations have been not confirmed in other reports [40]. Increased Ve was also reported to be associated with decreased PFS [120] and OS [40,114] with increasing values during treatment also negatively affecting the prognosis in DIPG [125]. As with CBV and Ktrans, a decrease in Ve has been identified as able to monitor radiochemotherapy [149] and antiangiogenic treatment effects on tumor vasculature [150]. Increased Vp was also associated with decreased OS [145] together with increased AUC, [40] with some authors reporting there to be a correlation of the latter with lower survival only in MGMT unmethylated tumors [153]. On the whole, as additionally confirmed by the meta-analysis conducted by Choi et al., the decrease in perfusion parameters derived from DSC and DCE has been shown to be useful in monitoring antiangiogenic treatment effects even with the caveat of not necessarily translating to a better prognosis [154]. ASL studies showed that CBF is a negative predictor of PFS [33,155] and OS [23]. Lower CBF also showed a trend for increased time to recurrence, despite not reaching statistical significance in a study by Qiao et al. [33]. A few PCT studies reported there to be an association between the perfusion parameters and prognosis. Increased PCT-derived CBV and decreased permeability area product were found to be associated with decreased OS [156–158].

3. Future Directions

3.1. New Approaches to Hemodynamic Imaging

The perfusion parameters and permeability parameters allow for the description of the pathophysiological characteristics of abnormal vasculature in the tumor, yet the lesional histopathological heterogeneity suggests that a more refined hemodynamic and metabolic assessment of the glioma features could better describe tumor type, aggressiveness, and prognosis through an enhanced characterization of the microvascular hemodynamic habitat (Figure 2).

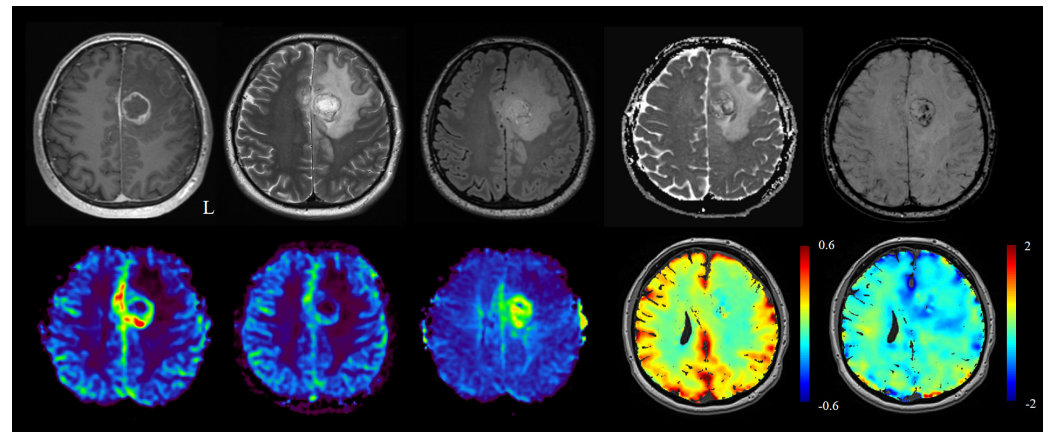


Figure 2. Standard MRI sequences, top row from left to right: T1 contrast-enhanced, T2, fluid attenuated inversion recovery (FLAIR), diffusion-weighted imaging (DWI), and susceptibility-weighted imaging (SWI). Perfusion MRI and advanced sequences, bottom row from left to right: CBV, CBF, MTT, BOLD-cerebrovascular reactivity (CVR), and hypoxia-enhanced BOLD MRI.

A few exemplary studies supporting this concept are now presented. Stadlbauer et al. applied a multiparametric MRI approach focusing on microvascular architecture including parameters such as microvascular density, vessel size index (VSI i.e., microvessel radius), neovascular activity (MTI, microvessel type indicator), and oxygen metabolism i.e., oxygen extraction fraction (OEF), cerebral metabolic rate of oxygen (CMRO₂), and oxygen partial pressure (PO₂) (by means of quantitative blood-oxygen level dependent (BOLD) MRI). In their series of publications, they show that this approach is able to predict glioblastoma recurrence through the identification of early pathophysiological alterations [159]. The same approach was used to identify different patterns of tumor microenvironment based on oxygen metabolism and neovascularization which can correlate with prognosis and phenotype switching [160,161]. As shown by the Garcia-Gomez group, the standardization of perfusion imaging and the correlation of imaging features can be integrated into standardized software-based ML-aided analysis for the determination of a refined “hemodynamic signature” (<https://www.oncohabitats.upv.es/> Last accessed on 21 December 2021), i.e., of the microvascular habitat, as part of the identification of diffuse glioma regarding both the enhanced tumor and edema [134] with important prognostic implications [162,163] to integrate with other known molecular prognostic markers [62,164] and the potential to provide insight on treatment strategy refinements [165]. External validations of this pipeline, even if still based on modest sample sizes, have provided encouraging results [20,163] and support similar efforts in this direction.

3.2. Contrast-Enhanced Ultrasound (CEUS)

Intraoperative CE ultrasound (CEUS) has been also gaining attention for the intraoperative assessment of tumor vasculature [166]. This technique exploits special microbubble-based contrast agents to visualize the tumor vasculature. It is safe, repeatable, correlates to MRI findings of contrast-enhancement, [167] and it can be used to improve the extent of resection by identifying any residual tumor [166,168,169]. Moreover, through the means

of perfusion assessment, the glioma grade can be predicted [170–172]. With respect of the techniques used to monitor CBF intra-operatively that are increasingly reported [173], these have been recently reviewed by Tahhan et al. [174].

3.3. Intravoxel Incoherent Motion (IVIM)-MRI

Based on a model proposed by Le Bihan et al. in the late 80s [175,176], IVIM-MRI was introduced as a diffusion-based method able to extract quantitative local microvascular perfusion information without the need for a contrast agent (see the review by Federau for further details) [177]. This technique yields three parameters, i.e., perfusion fraction (f) which is a measure proportional to CBV, pseudodiffusion coefficient (D^*), and blood-flow related parameters fD^* , and it has been the focus of brain tumor research as well. Similar to traditional hemodynamic imaging, IVIM-MRI has been also used for differential diagnosis (perfusion fraction is increased in high-grade compared with low-grade gliomas, and it allows for the differentiation of cerebral lymphomas—lower f versus high-grade glioma) [178–180], glioma grading, and IDH mutation prediction [181–184] to monitor the treatment effects [185–187], to identify tumor progression [109], and to predict survival [188–190].

3.4. Gas Modulation and BOLD Imaging: BOLD-CVR and Oxygen Modulation for Enhanced Lesion Characterization

The basic model underlying cerebrovascular reactivity has been addressed in Part A of the present review. As mentioned, in recent years, BOLD-cerebrovascular reactivity (CVR) has also been developed and intensively investigated in diffuse gliomas. Preliminary studies under breath-holding stimuli have revealed that the physiological cerebrovascular response is impaired in diffuse cerebral glioma patients possibly due to the altered vascular response in tumor tissue resulting in flow redistribution and the steal phenomenon [191,192]. CVR mapping has been also used to assess neurovascular uncoupling [193]. As previously introduced, the refinements in gas modulation control have provided better reproducibility for the evaluation of CVR [194,195]. Some of the recent studies exploiting this advantage have provided insights into glioma hemodynamic. CVR is in fact altered in areas of high-grade glioma recurrence [196] in the peritumoral tissue, with impairment confirmed by altered hemodynamic perfusion measures [197], and extending beyond the CE, FLAIR/T2, and hypermetabolism observed in positron emission tomography (PET) imaging [198]. Furthermore, BOLD-CVR has been able to elucidate remote changes in patients with gliomas such as a whole-brain decreased CVR suggesting global hemodynamic alterations [199] and the presence of crossed cerebellar diaschisis [200], and has shown the potential to distinguish radiation necrosis from glioblastoma [79]. Differential responses during separate oxygen and carbon dioxide modulation in the same tissue voxels may, in principle, hint at aberrant versus functional vasculature [201]. Interestingly, oxygen modulation has been also recently proposed as a means to study cerebral perfusion through rapid transient hemoglobin desaturation with the potential to substitute contrast-based perfusion [202–204] with advantages also relating to the avoidance of gadolinium contrast use [205], but application in the study of brain tumors is still lacking. Independently of these developments, the possibility of precise end-tidal oxygen modulation in isocapnic conditions has been preliminarily investigated as a means to provide a novel “imaging biomarker” to detail glioblastoma lesion microvascular features during BOLD imaging, exploiting hypoxia and hyperoxia as BOLD contrasts [206].

3.5. Machine-Learning and Radiomics

The new development of radiomics allows for the extraction of a high number of quantitative features to identify relations in the data that are not appreciable through traditional analytical methods [207,208]. Radiomics, and the possibility to combine it with machine learning algorithms, have shown considerable potential in terms of improving the diagnostic, prognostic, and predictive accuracy of conventional imaging analysis [207–210].

For example, every year, the Multimodal Brain Tumor Image Segmentation Benchmark (BRATS) challenge serves as a platform for developing better algorithms aimed at brain tumor segmentation. Other projects such as the REMBRANDT also make available genomics data of glioblastoma patients in conjunction with acquired imaging sequences annotated by expert neuroradiologists using the VASARI feature set [211,212]. This rapidly growing area of research has also adapted to using the data obtained from hemodynamic imaging modalities such as DSC [213], DCE [214], and ASL [215]. The use of perfusion imaging-derived radiomic features has shown promising feasibility in predicting MGMT promoter methylation [34] and IDH mutation status [216–219] and for improving the differential diagnosis of gliomas [220], the diagnostic performance of tumor grading [215,221] as well as pseudoprogression [222–224], but also prognostication [225]. Perfusional tumor heterogeneity can also be used to extract the radiomic features needed to train deep learning models for the prediction of glioblastoma recurrence patterns [226].

4. Conclusions

Advanced hemodynamic imaging research has provided yet another promising imaging development to complement traditional tumor grading by correlating the specific hemodynamic patterns posed by diffuse glioma to molecular and pathophysiological alterations. Despite promising associations being found, the evidence remains overall scarce and often conflicting with traditional histopathological and immunohistochemical analysis remaining the gold standard for diffuse cerebral glioma diagnosis. The monitoring of treatment effects and the differentiation of tumor progression/recurrence from treatment-induced changes can benefit significantly from hemodynamic imaging. The present literature points out the encouraging results for this purpose with the caveat that the lack of acquisition and processing standardization still limits its reliability for diffuse clinical integration. The identification of hemodynamic biomarkers correlated to prognosis can assist clinical management decisions and provide the basis for trial stratification to reveal missed patterns in connection to the treatment effects. As methodological optimization continues to be pursued, innovative hemodynamic imaging approaches are emerging with the potential to further advance the characterization of diffuse cerebral gliomas pre-operatively and during the follow-up by overcoming known technical limitations. The integration of radiomics and machine learning in the analysis pipeline can further extend the diagnostic and prognostic potential of hemodynamic imaging in cerebral diffuse glioma.

Author Contributions: Conceptualization, V.S., L.G. and J.F.; methodology, V.S., L.G., J.B. and J.F.; formal analysis, V.S. and L.G.; investigation, V.S. and L.G.; resources, V.S., L.G. and J.F.; data curation, V.S. and L.G.; writing—original draft preparation, V.S., L.G., J.B. and J.F.; writing—review and editing, V.S., L.G., J.B., C.H.B.V.N., M.S., M.B., A.B., M.W., Z.K., L.R. and J.F.; visualization, V.S. and J.B.; supervision, J.F.; funding acquisition, J.F. All authors have read and agreed to the published version of the manuscript.

Funding: This research was funded by Swiss Cancer League, KFS-3975-08-2016-R.

Conflicts of Interest: The authors declare no conflict of interest. The funders had no role in the design of the study; in the collection, analyses, or interpretation of data; in the writing of the manuscript, or in the decision to publish the results.

References

1. Ludwig, K.; Kornblum, H.I. Molecular markers in glioma. *J. Neuro Oncol.* **2017**, *134*, 505–512. [[CrossRef](#)] [[PubMed](#)]
2. Louis, D.N.; Perry, A.; Wesseling, P.; Brat, D.J.; Cree, I.A.; Figarella-Branger, D.; Hawkins, C.; Ng, H.K.; Pfister, S.M.; Reifenberger, G.; et al. The 2021 WHO Classification of Tumors of the Central Nervous System: A summary. *Neuro Oncol.* **2021**, *23*, 1231–1251. [[CrossRef](#)] [[PubMed](#)]
3. Weller, M.; van den Bent, M.; Preusser, M.; Le Rhun, E.; Tonn, J.C.; Minniti, G.; Bendszus, M.; Balana, C.; Chinot, O.; Dirven, L.; et al. EANO guidelines on the diagnosis and treatment of diffuse gliomas of adulthood. *Nat. Rev. Clin. Oncol.* **2020**, *18*, 170–186. [[CrossRef](#)] [[PubMed](#)]
4. Smits, M.; van den Bent, M.J. Imaging Correlates of Adult Glioma Genotypes. *Radiology* **2017**, *284*, 316–331. [[CrossRef](#)]

5. Zikou, A.; Sioka, C.; Alexiou, G.A.; Fotopoulos, A.; Voulgaris, S.; Argyropoulou, M.I. Radiation Necrosis, Pseudoprogression, Pseudoresponse, and Tumor Recurrence: Imaging Challenges for the Evaluation of Treated Gliomas. *Contrast Media Mol. Imaging* **2018**, *2018*, e6828396. [[CrossRef](#)]
6. Guida, L.; Stumpo, V.; Bellomo, J.; van Niftrik, C.H.B.; Sebök, M.; Berhouma, M.; Bink, A.; Weller, M.; Kulcsar, Z.; Regli, L.; et al. Hemodynamic Imaging in Cerebral Diffuse Glioma—Part A: Concept, Differential Diagnosis and Tumor Grading. *Cancers* **2022**. *manuscript under peer review*.
7. Phillip Law, W.; Miles, K.A. Incorporating prognostic imaging biomarkers into clinical practice. *Cancer Imaging* **2013**, *13*, 332–341. [[CrossRef](#)]
8. Sanvito, F.; Castellano, A.; Falini, A. Advancements in Neuroimaging to Unravel Biological and Molecular Features of Brain Tumors. *Cancers* **2021**, *13*, 424. [[CrossRef](#)]
9. Shui, L.; Ren, H.; Yang, X.; Li, J.; Chen, Z.; Yi, C.; Zhu, H.; Shui, P. The Era of Radiogenomics in Precision Medicine: An Emerging Approach to Support Diagnosis, Treatment Decisions, and Prognostication in Oncology. *Front. Oncol.* **2021**, *10*, 3195. [[CrossRef](#)]
10. Song, S.; Wang, L.; Yang, H.; Shan, Y.; Cheng, Y.; Xu, L.; Dong, C.; Zhao, G.; Lu, J. Static 18F-FET PET and DSC-PWI based on hybrid PET/MR for the prediction of gliomas defined by IDH and 1p/19q status. *Eur. Radiol.* **2020**, *31*, 4087–4096. [[CrossRef](#)]
11. Conte, G.M.; Altabella, L.; Castellano, A.; Cuccarini, V.; Bizzi, A.; Grimaldi, M.; Costa, A.; Caulo, M.; Falini, A.; Anzalone, N. Comparison of T1 mapping and fixed T1 method for dynamic contrast-enhanced MRI perfusion in brain gliomas. *Eur. Radiol.* **2019**, *29*, 3467–3479. [[CrossRef](#)]
12. Wang, N.; Xie, S.; Liu, H.; Chen, G.; Zhang, W. Arterial Spin Labeling for Glioma Grade Discrimination: Correlations with IDH1 Genotype and 1p/19q Status. *Transl. Oncol.* **2019**, *12*, 749–756. [[CrossRef](#)] [[PubMed](#)]
13. Arevalo-Perez, J.; Peck, K.K.; Young, R.J.; Holodny, A.I.; Karimi, S.; Lyo, J.K. Dynamic Contrast-Enhanced Perfusion MRI and Diffusion-Weighted Imaging in Grading of Gliomas. *J. Neuroimaging* **2015**, *25*, 792–798. [[CrossRef](#)] [[PubMed](#)]
14. Fudaba, H.; Shimomura, T.; Abe, T.; Matsuta, H.; Momii, Y.; Sugita, K.; Ooba, H.; Kamida, T.; Hikawa, T.; Fujiki, M. Comparison of Multiple Parameters Obtained on 3T Pulsed Arterial Spin-Labeling, Diffusion Tensor Imaging, and MRS and the Ki-67 Labeling Index in Evaluating Glioma Grading. *Am. J. Neuroradiol.* **2014**, *35*, 2091–2098. [[CrossRef](#)]
15. Alexiou, G.A.; Zikou, A.; Tsiouris, S.; Goussia, A.; Kosta, P.; Papadopoulos, A.; Voulgaris, S.; Kyritsis, A.P.; Fotopoulos, A.D.; Argyropoulou, M.I. Correlation of diffusion tensor, dynamic susceptibility contrast MRI and 99mTc-Tetrofosmin brain SPECT with tumour grade and Ki-67 immunohistochemistry in glioma. *Clin. Neurol. Neurosurg.* **2014**, *116*, 41–45. [[CrossRef](#)]
16. Awasthi, R.; Rathore, R.K.S.; Soni, P.; Sahoo, P.; Awasthi, A.; Husain, N.; Behari, S.; Singh, R.K.; Pandey, C.M.; Gupta, R.K. Discriminant analysis to classify glioma grading using dynamic contrast-enhanced MRI and immunohistochemical markers. *Neuroradiology* **2012**, *54*, 205–213. [[CrossRef](#)]
17. Emblem, K.E.; Scheie, D.; Due-Tønnessen, P.; Nedregaard, B.; Nome, T.; Hald, J.K.; Beiske, K.; Meling, T.R.; Bjørnerud, A. Histogram Analysis of MR Imaging–Derived Cerebral Blood Volume Maps: Combined Glioma Grading and Identification of Low-Grade Oligodendroglial Subtypes. *Am. J. Neuroradiol.* **2008**, *29*, 1664–1670. [[CrossRef](#)]
18. Tateishi, K.; Tateishi, U.; Sato, M.; Yamanaka, S.; Kanno, H.; Murata, H.; Inoue, T.; Kawahara, N. Application of 62Cu-Diacetyl-Bis (N4-Methylthiosemicarbazone) PET Imaging to Predict Highly Malignant Tumor Grades and Hypoxia-Inducible Factor-1 α Expression in Patients with Glioma. *Am. J. Neuroradiol.* **2013**, *34*, 92–99. [[CrossRef](#)] [[PubMed](#)]
19. Mao, J.; Deng, D.; Yang, Z.; Wang, W.; Cao, M.; Huang, Y.; Shen, J. Pretreatment structural and arterial spin labeling MRI is predictive for p53 mutation in high-grade gliomas. *Br. J. Radiol.* **2020**, *93*, 20200661. [[CrossRef](#)] [[PubMed](#)]
20. Wu, H.; Tong, H.; Du, X.; Guo, H.; Ma, Q.; Zhang, Y.; Zhou, X.; Liu, H.; Wang, S.; Fang, J.; et al. Vascular habitat analysis based on dynamic susceptibility contrast perfusion MRI predicts IDH mutation status and prognosis in high-grade gliomas. *Eur. Radiol.* **2020**, *30*, 3254–3265. [[CrossRef](#)]
21. Xue, W.; Zhang, J.; Tong, H.; Xie, T.; Chen, X.; Zhou, B.; Wu, P.; Zhong, P.; Du, X.; Guo, Y.; et al. Effects of BMPER, CXCL10, and HOXA9 on Neovascularization During Early-Growth Stage of Primary High-Grade Glioma and Their Corresponding MRI Biomarkers. *Front. Oncol.* **2020**, *10*, 10. [[CrossRef](#)] [[PubMed](#)]
22. Piccardo, A.; Tortora, D.; Mascelli, S.; Severino, M.; Piatelli, G.; Consales, A.; Pescetto, M.; Biassoni, V.; Schiavello, E.; Massollo, M.; et al. Advanced MR imaging and 18F-DOPA PET characteristics of H3K27M-mutant and wild-type pediatric diffuse midline gliomas. *Eur. J. Nucl. Med. Mol. Imaging* **2019**, *46*, 1685–1694. [[CrossRef](#)] [[PubMed](#)]
23. Pang, H.; Dang, X.; Ren, Y.; Zhuang, D.; Qiu, T.; Chen, H.; Zhang, J.; Ma, N.; Li, G.; Zhang, J.; et al. 3D-ASL perfusion correlates with VEGF expression and overall survival in glioma patients: Comparison of quantitative perfusion and pathology on accurate spatial location-matched basis. *J. Magn. Reson. Imaging* **2019**, *50*, 209–220. [[CrossRef](#)] [[PubMed](#)]
24. Bekaert, L.; Valable, S.; Lechapt-Zalcman, E.; Ponte, K.; Collet, S.; Constans, J.-M.; Levallet, G.; Bordji, K.; Petit, E.; Branger, P.; et al. [18F]-FMISO PET study of hypoxia in gliomas before surgery: Correlation with molecular markers of hypoxia and angiogenesis. *Eur. J. Nucl. Med. Mol. Imaging* **2017**, *44*, 1383–1392. [[CrossRef](#)]
25. Haris, M.; Husain, N.; Singh, A.; Husain, M.; Srivastava, S.; Srivastava, C.; Behari, S.; Rathore, R.K.S.; Saksena, S.; Gupta, R.K. Dynamic Contrast-Enhanced Derived Cerebral Blood Volume Correlates Better With Leak Correction Than With No Correction for Vascular Endothelial Growth Factor, Microvascular Density, and Grading of Astrocytoma. *J. Comput. Assist. Tomogr.* **2008**, *32*, 955–965. [[CrossRef](#)]

26. Maia, A.C.M.; Malheiros, S.M.F.; da Rocha, A.J.; da Silva, C.J.; Gabbai, A.A.; Ferraz, F.A.P.; Stávale, J.N. MR Cerebral Blood Volume Maps Correlated with Vascular Endothelial Growth Factor Expression and Tumor Grade in Nonenhancing Gliomas. *Am. J. Neuroradiol.* **2005**, *26*, 777–783.
27. Li, X.; Vigneron, D.B.; Cha, S.; Graves, E.E.; Crawford, F.; Chang, S.M.; Nelson, S.J. Relationship of MR-Derived Lactate, Mobile Lipids, and Relative Blood Volume for Gliomas In Vivo. *Am. J. Neuroradiol.* **2005**, *26*, 760–769.
28. Aronen, H.J.; Gazit, I.E.; Louis, D.N.; Buchbinder, B.R.; Pardo, F.S.; Weisskoff, R.M.; Harsh, G.R.; Cosgrove, G.R.; Halpern, E.F.; Hochberg, F.H. Cerebral blood volume maps of gliomas: Comparison with tumor grade and histologic findings. *Radiology* **1994**, *191*, 41–51. [[CrossRef](#)]
29. Kickingeder, P.; Sahm, F.; Radbruch, A.; Wick, W.; Heiland, S.; von Deimling, A.; Bendszus, M.; Wiestler, B. IDH mutation status is associated with a distinct hypoxia/angiogenesis transcriptome signature which is non-invasively predictable with rCBV imaging in human glioma. *Sci. Rep.* **2015**, *5*, 16238. [[CrossRef](#)]
30. Hong, E.K.; Choi, S.H.; Shin, D.J.; Jo, S.W.; Yoo, R.-E.; Kang, K.M.; Yun, T.J.; Kim, J.; Sohn, C.-H.; Park, S.-H.; et al. Comparison of Genetic Profiles and Prognosis of High-Grade Gliomas Using Quantitative and Qualitative MRI Features: A Focus on G3 Gliomas. *Korean J. Radiol.* **2021**, *22*, 233–242. [[CrossRef](#)]
31. Ahn, S.S.; Shin, N.-Y.; Chang, J.H.; Kim, S.H.; Kim, E.H.; Kim, D.W.; Lee, S.-K. Prediction of methylguanine methyltransferase promoter methylation in glioblastoma using dynamic contrast-enhanced magnetic resonance and diffusion tensor imaging: Clinical article. *J. Neurosurg.* **2014**, *121*, 367–373. [[CrossRef](#)] [[PubMed](#)]
32. Lee, S.; Choi, S.H.; Ryoo, L.; Yoon, T.J.; Kim, T.M.; Lee, S.-H.; Park, C.-K.; Kim, J.-H.; Sohn, C.-H.; Park, S.-H.; et al. Evaluation of the microenvironmental heterogeneity in high-grade gliomas with IDH1/2 gene mutation using histogram analysis of diffusion-weighted imaging and dynamic-susceptibility contrast perfusion imaging. *J. Neuro Oncol.* **2015**, *121*, 141–150. [[CrossRef](#)] [[PubMed](#)]
33. Qiao, X.J.; Ellingson, B.M.; Kim, H.J.; Wang, D.J.J.; Salamon, N.; Linetsky, M.; Sepahdari, A.R.; Jiang, B.; Tian, J.J.; Esswein, S.R.; et al. Arterial Spin-Labeling Perfusion MRI Stratifies Progression-Free Survival and Correlates with Epidermal Growth Factor Receptor Status in Glioblastoma. *Am. J. Neuroradiol.* **2015**, *36*, 672–677. [[CrossRef](#)] [[PubMed](#)]
34. Crisi, G.; Filice, S. Predicting MGMT Promoter Methylation of Glioblastoma from Dynamic Susceptibility Contrast Perfusion: A Radiomic Approach. *J. Neuroimaging* **2020**, *30*, 458–462. [[CrossRef](#)]
35. Choi, H.J.; Choi, S.H.; You, S.-H.; Yoo, R.-E.; Kang, K.M.; Yun, T.J.; Kim, J.-H.; Sohn, C.-H.; Park, C.-K.; Park, S.-H. MGMT Promoter Methylation Status in Initial and Recurrent Glioblastoma: Correlation Study with DWI and DSC PWI Features. *Am. J. Neuroradiol.* **2021**, *42*, 853–860. [[CrossRef](#)]
36. Waitkus, M.S.; Diplas, B.H.; Yan, H. Isocitrate dehydrogenase mutations in gliomas. *Neuro Oncol.* **2016**, *18*, 16–26. [[CrossRef](#)]
37. Yamashita, A.S.; da Costa Rosa, M.; Stumpo, V.; Rais, R.; Slusher, B.S.; Riggins, G.J. The glutamine antagonist prodrug JHU-083 slows malignant glioma growth and disrupts mTOR signaling. *Neuro Oncol. Adv.* **2021**, *3*, vdaa149. [[CrossRef](#)]
38. Xing, Z.; Yang, X.; She, D.; Lin, Y.; Zhang, Y.; Cao, D. Noninvasive Assessment of IDH Mutational Status in World Health Organization Grade II and III Astrocytomas Using DWI and DSC-PWI Combined with Conventional MR Imaging. *Am. J. Neuroradiol.* **2017**, *38*, 1138–1144. [[CrossRef](#)]
39. Tan, W.; Xiong, J.; Huang, W.; Wu, J.; Zhan, S.; Geng, D. Noninvasively detecting Isocitrate dehydrogenase 1 gene status in astrocytoma by dynamic susceptibility contrast MRI. *J. Magn. Reson. Imaging* **2017**, *45*, 492–499. [[CrossRef](#)]
40. Cindil, E.; Sendur, H.N.; Cerit, M.N.; Erdogan, N.; Celebi, F.; Dag, N.; Celtikci, E.; Inan, A.; Oner, Y.; Tali, T. Prediction of IDH Mutation Status in High-grade Gliomas Using DWI and High T1-weight DSC-MRI. *Acad. Radiol.* **2021**. *online ahead of print.* [[CrossRef](#)]
41. Zhang, H.; Iyu, G.; He, W.; Lei, Y.; Lin, F.; Wang, M.; Zhang, H.; Liang, L.; Feng, Y.; Yang, J. DSC and DCE Histogram Analyses of Glioma Biomarkers, Including IDH, MGMT, and TERT, on Differentiation and Survival. *Acad. Radiol.* **2020**, *27*, e263–e271. [[CrossRef](#)] [[PubMed](#)]
42. Li, Z.; Zhao, W.; He, B.; Koh, T.S.; Li, Y.; Zeng, Y.; Zhang, Z.; Zhang, J.; Hou, Z. Application of Distributed Parameter Model to Assessment of Glioma IDH Mutation Status by Dynamic Contrast-Enhanced Magnetic Resonance Imaging. Available online: <https://www.hindawi.com/journals/cmmi/2020/8843084/> (accessed on 14 December 2021).
43. Brendle, C.; Hempel, J.-M.; Schittenhelm, J.; Skardelly, M.; Tabatabai, G.; Bender, B.; Ernemann, U.; Klose, U. Glioma Grading and Determination of IDH Mutation Status and ATRX loss by DCE and ASL Perfusion. *Clin. Neuroradiol.* **2018**, *28*, 421–428. [[CrossRef](#)] [[PubMed](#)]
44. Yoo, R.-E.; Yun, T.J.; Hwang, I.; Hong, E.K.; Kang, K.M.; Choi, S.H.; Park, C.-K.; Won, J.-K.; Kim, J.; Sohn, C.-H. Arterial spin labeling perfusion-weighted imaging aids in prediction of molecular biomarkers and survival in glioblastomas. *Eur. Radiol.* **2020**, *30*, 1202–1211. [[CrossRef](#)]
45. Wang, K.; Li, Y.; Cheng, H.; Li, S.; Xiang, W.; Ming, Y.; Chen, L.; Zhou, J. Perfusion CT detects alterations in local cerebral flow of glioma related to IDH, MGMT and TERT status. *BMC Neurol.* **2021**, *21*, 460. [[CrossRef](#)] [[PubMed](#)]
46. Polívka, J., Jr.; Pešta, M.; Pitule, P.; Hes, O.; Holubec, L.; Polívka, J.; Kubíková, T.; Tonar, Z. IDH1 mutation is associated with lower expression of VEGF but not microvessel formation in glioblastoma multiforme. *Oncotarget* **2018**, *9*, 16462–16476. [[CrossRef](#)]
47. Bou Zerdan, M.; Assi, H.I. Oligodendroglioma: A Review of Management and Pathways. *Front. Mol. Neurosci.* **2021**, *14*, 225. [[CrossRef](#)]

48. Latysheva, A.; Emblem, K.E.; Brandal, P.; Vik-Mo, E.O.; Pahnke, J.; Røysland, K.; Hald, J.K.; Server, A. Dynamic susceptibility contrast and diffusion MR imaging identify oligodendroglioma as defined by the 2016 WHO classification for brain tumors: Histogram analysis approach. *Neuroradiology* **2019**, *61*, 545–555. [[CrossRef](#)]
49. Mair, M.J.; Geurts, M.; van den Bent, M.J.; Berghoff, A.S. A basic review on systemic treatment options in WHO grade II-III gliomas. *Cancer Treat. Rev.* **2021**, *92*, 102124. [[CrossRef](#)]
50. Sunwoo, L.; Choi, S.H.; Yoo, R.-E.; Kang, K.M.; Yun, T.J.; Kim, T.M.; Lee, S.-H.; Park, C.-K.; Kim, J.; Park, S.-W.; et al. Paradoxical perfusion metrics of high-grade gliomas with an oligodendroglioma component: Quantitative analysis of dynamic susceptibility contrast perfusion MR imaging. *Neuroradiology* **2015**, *57*, 1111–1120. [[CrossRef](#)]
51. Lee, J.Y.; Ahn, K.J.; Lee, Y.S.; Jang, J.H.; Jung, S.L.; Kim, B.S. Differentiation of grade II and III oligodendrogliomas from grade II and III astrocytomas: A histogram analysis of perfusion parameters derived from dynamic contrast-enhanced (DCE) and dynamic susceptibility contrast (DSC) MRI. *Acta Radiol.* **2018**, *59*, 723–731. [[CrossRef](#)]
52. Yoon, H.J.; Ahn, K.J.; Lee, S.; Jang, J.H.; Choi, H.S.; Jung, S.L.; Kim, B.S.; Jeun, S.S.; Hong, Y.K. Differential diagnosis of oligodendroglial and astrocytic tumors using imaging results: The added value of perfusion MR imaging. *Neuroradiology* **2017**, *59*, 665–675. [[CrossRef](#)] [[PubMed](#)]
53. Delgado, A.F.; Delgado, A.F. Discrimination between Glioma Grades II and III Using Dynamic Susceptibility Perfusion MRI: A Meta-Analysis. *Am. J. Neuroradiol.* **2017**, *38*, 1348–1355. [[CrossRef](#)] [[PubMed](#)]
54. Narang, J.; Jain, R.; Scarpace, L.; Saksena, S.; Schultz, L.R.; Rock, J.P.; Rosenblum, M.; Patel, S.C.; Mikkelsen, T. Tumor vascular leakiness and blood volume estimates in oligodendrogliomas using perfusion CT: An analysis of perfusion parameters helping further characterize genetic subtypes as well as differentiate from astroglial tumors. *J. Neurooncol.* **2011**, *102*, 287–293. [[CrossRef](#)] [[PubMed](#)]
55. Mansouri, A.; Hachem, L.D.; Mansouri, S.; Nassiri, F.; Laperriere, N.J.; Xia, D.; Lindeman, N.I.; Wen, P.Y.; Chakravarti, A.; Mehta, M.P.; et al. MGMT promoter methylation status testing to guide therapy for glioblastoma: Refining the approach based on emerging evidence and current challenges. *Neuro Oncol.* **2019**, *21*, 167–178. [[CrossRef](#)]
56. Moon, W.-J.; Choi, J.W.; Roh, H.G.; Lim, S.D.; Koh, Y.-C. Imaging parameters of high grade gliomas in relation to the MGMT promoter methylation status: The CT, diffusion tensor imaging, and perfusion MR imaging. *Neuroradiology* **2012**, *54*, 555–563. [[CrossRef](#)]
57. Han, Y.; Yan, L.-F.; Wang, X.-B.; Sun, Y.-Z.; Zhang, X.; Liu, Z.-C.; Nan, H.-Y.; Hu, Y.-C.; Yang, Y.; Zhang, J.; et al. Structural and advanced imaging in predicting MGMT promoter methylation of primary glioblastoma: A region of interest based analysis. *BMC Cancer* **2018**, *18*, 215. [[CrossRef](#)]
58. Mikkelsen, V.E.; Dai, H.Y.; Stensjøen, A.L.; Berntsen, E.M.; Salvesen, Ø.; Solheim, O.; Torp, S.H. MGMT Promoter Methylation Status Is Not Related to Histological or Radiological Features in IDH Wild-type Glioblastomas. *J. Neuropathol. Exp. Neurol.* **2020**, *79*, 855–862. [[CrossRef](#)]
59. Ozturk, K.; Soylu, E.; Cayci, Z. Correlation between dynamic susceptibility contrast perfusion MRI and genomic alterations in glioblastoma. *Neuroradiology* **2021**, *63*, 1801–1810. [[CrossRef](#)]
60. Lu, J.; Li, X.; Li, H. Perfusion parameters derived from MRI for preoperative prediction of IDH mutation and MGMT promoter methylation status in glioblastomas. *Magn. Reson. Imaging* **2021**, *83*, 189–195. [[CrossRef](#)]
61. Ryoo, I.; Choi, S.H.; Kim, J.-H.; Sohn, C.-H.; Kim, S.C.; Shin, H.S.; Yeom, J.A.; Jung, S.C.; Lee, A.L.; Yun, T.J.; et al. Cerebral Blood Volume Calculated by Dynamic Susceptibility Contrast-Enhanced Perfusion MR Imaging: Preliminary Correlation Study with Glioblastoma Genetic Profiles. *PLoS ONE* **2013**, *8*, e71704. [[CrossRef](#)]
62. Fuster-Garcia, E.; Lorente Estellés, D.; Álvarez-Torres, M.D.M.; Juan-Albarracín, J.; Chelebian, E.; Rovira, A.; Acosta, C.A.; Pineda, J.; Oleaga, L.; Mollá-Olmos, E.; et al. MGMT methylation may benefit overall survival in patients with moderately vascularized glioblastomas. *Eur. Radiol.* **2021**, *31*, 1738–1747. [[CrossRef](#)] [[PubMed](#)]
63. Oprita, A.; Baloi, S.-C.; Staicu, G.-A.; Alexandru, O.; Tache, D.E.; Danoiu, S.; Micu, E.S.; Sevastre, A.-S. Updated Insights on EGFR Signaling Pathways in Glioma. *Int. J. Mol. Sci.* **2021**, *22*, 587. [[CrossRef](#)]
64. Eskilsson, E.; Røsland, G.V.; Solecki, G.; Wang, Q.; Harter, P.N.; Graziani, G.; Verhaak, R.G.W.; Winkler, F.; Bjerkvig, R.; Miletic, H. EGFR heterogeneity and implications for therapeutic intervention in glioblastoma. *Neuro Oncol.* **2018**, *20*, 743–752. [[CrossRef](#)]
65. Gupta, A.; Young, R.J.; Shah, A.D.; Schweitzer, A.D.; Graber, J.J.; Shi, W.; Zhang, Z.; Huse, J.; Omuro, A.M.P. Pretreatment Dynamic Susceptibility Contrast MRI Perfusion in Glioblastoma: Prediction of EGFR Gene Amplification. *Clin. Neuroradiol.* **2015**, *25*, 143–150. [[CrossRef](#)] [[PubMed](#)]
66. Arevalo-Perez, J.; Thomas, A.A.; Kaley, T.; Lyo, J.; Peck, K.K.; Holodny, A.I.; Mellinghoff, I.K.; Shi, W.; Zhang, Z.; Young, R.J. T1-Weighted Dynamic Contrast-Enhanced MRI as a Noninvasive Biomarker of Epidermal Growth Factor Receptor vIII Status. *Am. J. Neuroradiol.* **2015**, *36*, 2256–2261. [[CrossRef](#)]
67. Tykocinski, E.S.; Grant, R.A.; Kapoor, G.S.; Krejza, J.; Bohman, L.-E.; Gocke, T.A.; Chawla, S.; Halpern, C.H.; Lopinto, J.; Melhem, E.R.; et al. Use of magnetic perfusion-weighted imaging to determine epidermal growth factor receptor variant III expression in glioblastoma. *Neuro Oncol.* **2012**, *14*, 613–623. [[CrossRef](#)]
68. Oughourlian, T.C.; Yao, J.; Hagiwara, A.; Nathanson, D.A.; Raymond, C.; Pope, W.B.; Salamon, N.; Lai, A.; Ji, M.; Nghiemphu, P.L.; et al. Relative oxygen extraction fraction (rOEF) MR imaging reveals higher hypoxia in human epidermal growth factor receptor (EGFR) amplified compared with non-amplified gliomas. *Neuroradiology* **2021**, *63*, 857–868. [[CrossRef](#)] [[PubMed](#)]

69. Hino-Shishikura, A.; Tateishi, U.; Shibata, H.; Yoneyama, T.; Nishii, T.; Torii, I.; Tateishi, K.; Ohtake, M.; Kawahara, N.; Inoue, T. Tumor hypoxia and microscopic diffusion capacity in brain tumors: A comparison of ⁶²Cu-Diacetyl-Bis (N4-Methylthiosemicarbazone) PET/CT and diffusion-weighted MR imaging. *Eur. J. Nucl. Med. Mol. Imaging* **2014**, *41*, 1419–1427. [[CrossRef](#)]
70. Jensen, R.L.; Mumert, M.L.; Gillespie, D.L.; Kinney, A.Y.; Schabel, M.C.; Salzman, K.L. Preoperative dynamic contrast-enhanced MRI correlates with molecular markers of hypoxia and vascularity in specific areas of intratumoral microenvironment and is predictive of patient outcome. *Neuro Oncol.* **2014**, *16*, 280–291. [[CrossRef](#)]
71. Liu, X.; Mangla, R.; Tian, W.; Qiu, X.; Li, D.; Walter, K.A.; Ekholm, S.; Johnson, M.D. The preliminary radiogenomics association between MR perfusion imaging parameters and genomic biomarkers, and their predictive performance of overall survival in patients with glioblastoma. *J. Neurooncol.* **2017**, *135*, 553–560. [[CrossRef](#)]
72. Strauss, S.B.; Meng, A.; Ebani, E.J.; Chiang, G.C. Imaging Glioblastoma Posttreatment: Progression, Pseudoprogression, Pseudoreponse, Radiation Necrosis. *Radiol. Clin. N. Am.* **2019**, *57*, 1199–1216. [[CrossRef](#)] [[PubMed](#)]
73. Thust, S.C.; van den Bent, M.J.; Smits, M. Pseudoprogression of brain tumors. *J. Magn. Reson. Imaging* **2018**, *48*, 571–589. [[CrossRef](#)] [[PubMed](#)]
74. Leao, D.J.; Craig, P.G.; Godoy, L.F.; Leite, C.C.; Policeni, B. Response Assessment in Neuro-Oncology Criteria for Gliomas: Practical Approach Using Conventional and Advanced Techniques. *Am. J. Neuroradiol.* **2020**, *41*, 10–20. [[CrossRef](#)] [[PubMed](#)]
75. Li, M.; Ren, X.; Dong, G.; Wang, J.; Jiang, H.; Yang, C.; Zhao, X.; Zhu, Q.; Cui, Y.; Yu, K.; et al. Distinguishing Pseudoprogression From True Early Progression in Isocitrate Dehydrogenase Wild-Type Glioblastoma by Interrogating Clinical, Radiological, and Molecular Features. *Front. Oncol.* **2021**, *11*, 601. [[CrossRef](#)]
76. Farid, N.; Almeida-Freitas, D.B.; White, N.S.; McDonald, C.R.; Kuperman, J.M.; Almutairi, A.A.; Muller, K.A.; VandenBerg, S.R.; Kesari, S.; Dale, A.M. Combining diffusion and perfusion differentiates tumor from bevacizumab-related imaging abnormality (bria). *J. Neurooncol.* **2014**, *120*, 539–546. [[CrossRef](#)]
77. Muscas, G.; van Niftrik, C.H.B.; Sebök, M.; Della Puppa, A.; Seystahl, K.; Andratschke, N.; Brown, M.; Weller, M.; Regli, L.; Piccirelli, M.; et al. Distinct Cerebrovascular Reactivity Patterns for Brain Radiation Necrosis. *Cancers* **2021**, *13*, 1840. [[CrossRef](#)]
78. Pyatigorskaya, N.; Sgard, B.; Bertaux, M.; Yahia-Cherif, L.; Kas, A. Can FDG-PET/MR help to overcome limitations of sequential MRI and PET-FDG for differential diagnosis between recurrence/progression and radionecrosis of high-grade gliomas? *J. Neuroradiol.* **2020**. [[CrossRef](#)]
79. Qiao, Z.; Zhao, X.; Wang, K.; Zhang, Y.; Fan, D.; Yu, T.; Shen, H.; Chen, Q.; Ai, L. Utility of Dynamic Susceptibility Contrast Perfusion-Weighted MR Imaging and ¹¹C-Methionine PET/CT for Differentiation of Tumor Recurrence from Radiation Injury in Patients with High-Grade Gliomas. *Am. J. Neuroradiol.* **2019**, *40*, 253–259. [[CrossRef](#)]
80. Sacconi, B.; Raad, R.A.; Lee, J.; Fine, H.; Kondziolka, D.; Golfinos, J.G.; Babb, J.S.; Jain, R. Concurrent functional and metabolic assessment of brain tumors using hybrid PET/MR imaging. *J. Neurooncol.* **2016**, *127*, 287–293. [[CrossRef](#)]
81. Prager, A.J.; Martinez, N.; Beal, K.; Omuro, A.; Zhang, Z.; Young, R.J. Diffusion and Perfusion MRI to Differentiate Treatment-Related Changes Including Pseudoprogression from Recurrent Tumors in High-Grade Gliomas with Histopathologic Evidence. *Am. J. Neuroradiol.* **2015**, *36*, 877–885. [[CrossRef](#)]
82. Shin, K.E.; Ahn, K.J.; Choi, H.S.; Jung, S.L.; Kim, B.S.; Jeon, S.S.; Hong, Y.G. DCE and DSC MR perfusion imaging in the differentiation of recurrent tumour from treatment-related changes in patients with glioma. *Clin. Radiol.* **2014**, *69*, e264–e272. [[CrossRef](#)] [[PubMed](#)]
83. Alexiou, G.A.; Zikou, A.; Tsiouris, S.; Goussia, A.; Kosta, P.; Papadopoulos, A.; Voulgaris, S.; Tsekeris, P.; Kyritsis, A.P.; Fotopoulos, A.D.; et al. Comparison of diffusion tensor, dynamic susceptibility contrast MRI and ^{99m}Tc-Tetrofosmin brain SPECT for the detection of recurrent high-grade glioma. *Magn. Reson. Imaging* **2014**, *32*, 854–859. [[CrossRef](#)] [[PubMed](#)]
84. Seeger, A.; Braun, C.; Skardelly, M.; Paulsen, F.; Schittenhelm, J.; Ernemann, U.; Bisdas, S. Comparison of Three Different MR Perfusion Techniques and MR Spectroscopy for Multiparametric Assessment in Distinguishing Recurrent High-Grade Gliomas from Stable Disease. *Acad. Radiol.* **2013**, *20*, 1557–1565. [[CrossRef](#)] [[PubMed](#)]
85. Gahramanov, S.; Muldoon, L.L.; Varallyay, C.G.; Li, X.; Kraemer, D.F.; Fu, R.; Hamilton, B.E.; Rooney, W.D.; Neuwelt, E.A. Pseudoprogression of Glioblastoma after Chemo- and Radiation Therapy: Diagnosis by Using Dynamic Susceptibility-weighted Contrast-enhanced Perfusion MR Imaging with Ferumoxytol versus Gadoteridol and Correlation with Survival. *Radiology* **2013**, *266*, 842–852. [[CrossRef](#)]
86. Larsen, V.A.; Simonsen, H.J.; Law, I.; Larsson, H.B.W.; Hansen, A.E. Evaluation of dynamic contrast-enhanced T1-weighted perfusion MRI in the differentiation of tumor recurrence from radiation necrosis. *Neuroradiology* **2013**, *55*, 361–369. [[CrossRef](#)]
87. Baek, H.J.; Kim, H.S.; Kim, N.; Choi, Y.J.; Kim, Y.J. Percent Change of Perfusion Skewness and Kurtosis: A Potential Imaging Biomarker for Early Treatment Response in Patients with Newly Diagnosed Glioblastomas. *Radiology* **2012**, *264*, 834–843. [[CrossRef](#)]
88. Bisdas, S.; Naegele, T.; Ritz, R.; Dimostheni, A.; Pfannenber, C.; Reimold, M.; Koh, T.S.; Ernemann, U. Distinguishing Recurrent High-grade Gliomas from Radiation Injury: A Pilot Study Using Dynamic Contrast-enhanced MR Imaging. *Acad. Radiol.* **2011**, *18*, 575–583. [[CrossRef](#)]
89. Kim, Y.H.; Oh, S.W.; Lim, Y.J.; Park, C.-K.; Lee, S.-H.; Kang, K.W.; Jung, H.-W.; Chang, K.H. Differentiating radiation necrosis from tumor recurrence in high-grade gliomas: Assessing the efficacy of ¹⁸F-FDG PET, ¹¹C-methionine PET and perfusion MRI. *Clin. Neurol. Neurosurg.* **2010**, *112*, 758–765. [[CrossRef](#)]

90. Prat, R.; Galeano, I.; Lucas, A.; Martínez, J.C.; Martín, M.; Amador, R.; Reynés, G. Relative value of magnetic resonance spectroscopy, magnetic resonance perfusion, and 2-(18F) fluoro-2-deoxy-D-glucose positron emission tomography for detection of recurrence or grade increase in gliomas. *J. Clin. Neurosci.* **2010**, *17*, 50–53. [[CrossRef](#)]
91. Dandois, V.; Rommel, D.; Renard, L.; Jamart, J.; Cosnard, G. Substitution of 11C-methionine PET by perfusion MRI during the follow-up of treated high-grade gliomas: Preliminary results in clinical practice. *J. Neuroradiol.* **2010**, *37*, 89–97. [[CrossRef](#)]
92. Hu, L.S.; Baxter, L.C.; Smith, K.A.; Feuerstein, B.G.; Karis, J.P.; Eschbacher, J.M.; Coons, S.W.; Nakaji, P.; Yeh, R.F.; Debbins, J.; et al. Relative Cerebral Blood Volume Values to Differentiate High-Grade Glioma Recurrence from Posttreatment Radiation Effect: Direct Correlation between Image-Guided Tissue Histopathology and Localized Dynamic Susceptibility-Weighted Contrast-Enhanced Perfusion MR Imaging Measurements. *Am. J. Neuroradiol.* **2009**, *30*, 552–558. [[CrossRef](#)] [[PubMed](#)]
93. Barajas, R.F.; Chang, J.S.; Segal, M.R.; Parsa, A.T.; McDermott, M.W.; Berger, M.S.; Cha, S. Differentiation of Recurrent Glioblastoma Multiforme from Radiation Necrosis after External Beam Radiation Therapy with Dynamic Susceptibility-weighted Contrast-enhanced Perfusion MR Imaging. *Radiology* **2009**, *253*, 486–496. [[CrossRef](#)] [[PubMed](#)]
94. Sugahara, T.; Korogi, Y.; Kochi, M.; Ushio, Y.; Takahashi, M. Perfusion-sensitive MR Imaging of Gliomas: Comparison between Gradient-echo and Spin-echo Echo-planar Imaging Techniques. *Am. J. Neuroradiol.* **2001**, *22*, 1306–1315. [[PubMed](#)]
95. Hatzoglou, V.; Yang, T.J.; Omuro, A.; Gavrilovic, I.; Ulaner, G.; Rubel, J.; Schneider, T.; Woo, K.M.; Zhang, Z.; Peck, K.K.; et al. A prospective trial of dynamic contrast-enhanced MRI perfusion and fluorine-18 FDG PET-CT in differentiating brain tumor progression from radiation injury after cranial irradiation. *Neuro Oncol.* **2016**, *18*, 873–880. [[CrossRef](#)] [[PubMed](#)]
96. Yun, T.J.; Park, C.-K.; Kim, T.M.; Lee, S.-H.; Kim, J.-H.; Sohn, C.-H.; Park, S.-H.; Kim, I.H.; Choi, S.H. Glioblastoma Treated with Concurrent Radiation Therapy and Temozolomide Chemotherapy: Differentiation of True Progression from Pseudoprogression with Quantitative Dynamic Contrast-enhanced MR Imaging. *Radiology* **2014**, *274*, 830–840. [[CrossRef](#)] [[PubMed](#)]
97. Masch, W.R.; Wang, P.I.; Chenevert, T.L.; Junck, L.; Tsien, C.; Heth, J.A.; Sundgren, P.C. Comparison of Diffusion Tensor Imaging and Magnetic Resonance Perfusion Imaging in Differentiating Recurrent Brain Neoplasm From Radiation Necrosis. *Acad. Radiol.* **2016**, *23*, 569–576. [[CrossRef](#)]
98. Tsien, C.; Galbán, C.J.; Chenevert, T.L.; Johnson, T.D.; Hamstra, D.A.; Sundgren, P.C.; Junck, L.; Meyer, C.R.; Rehemtulla, A.; Lawrence, T.; et al. Parametric Response Map As an Imaging Biomarker to Distinguish Progression From Pseudoprogression in High-Grade Glioma. *J. Clin. Oncol.* **2010**, *28*, 2293–2299. [[CrossRef](#)]
99. Suh, C.H.; Kim, H.S.; Choi, Y.J.; Kim, N.; Kim, S.J. Prediction of Pseudoprogression in Patients with Glioblastomas Using the Initial and Final Area Under the Curves Ratio Derived from Dynamic Contrast-Enhanced T1-Weighted Perfusion MR Imaging. *Am. J. Neuroradiol.* **2013**, *34*, 2278–2286. [[CrossRef](#)]
100. Vöglein, J.; Tüttenberg, J.; Weimer, M.; Gerigk, L.; Kauczor, H.-U.; Essig, M.; Weber, M.-A. Treatment Monitoring in Gliomas: Comparison of Dynamic Susceptibility-Weighted Contrast-Enhanced and Spectroscopic MRI Techniques for Identifying Treatment Failure. *Investig. Radiol.* **2011**, *46*, 390–400. [[CrossRef](#)]
101. Hu, C.; Fang, X.; Hu, X.; Cui, L. Analysis of the mismatched manifestation between rCBF and rCBV maps in cerebral astrocytomas. *Clin. Imaging* **2009**, *33*, 417–423. [[CrossRef](#)]
102. Mangla, R.; Singh, G.; Ziegelitz, D.; Milano, M.T.; Korones, D.N.; Zhong, J.; Ekholm, S.E. Changes in Relative Cerebral Blood Volume 1 Month after Radiation-Temozolomide Therapy Can Help Predict Overall Survival in Patients with Glioblastoma. *Radiology* **2010**, *256*, 575–584. [[CrossRef](#)] [[PubMed](#)]
103. Iv, M.; Liu, X.; Lavezo, J.; Gentles, A.J.; Ghanem, R.; Lummus, S.; Born, D.E.; Soltys, S.G.; Nagpal, S.; Thomas, R.; et al. Perfusion MRI-Based Fractional Tumor Burden Differentiates between Tumor and Treatment Effect in Recurrent Glioblastomas and Informs Clinical Decision-Making. *Am. J. Neuroradiol.* **2019**, *40*, 1649–1657. [[CrossRef](#)] [[PubMed](#)]
104. Wang, L.; Wei, L.; Wang, J.; Li, N.; Gao, Y.; Ma, H.; Qu, X.; Zhang, M. Evaluation of perfusion MRI value for tumor progression assessment after glioma radiotherapy: A systematic review and meta-analysis. *Medicine* **2020**, *99*, e23766. [[CrossRef](#)] [[PubMed](#)]
105. Chuang, M.-T.; Liu, Y.-S.; Tsai, Y.-S.; Chen, Y.-C.; Wang, C.-K. Differentiating Radiation-Induced Necrosis from Recurrent Brain Tumor Using MR Perfusion and Spectroscopy: A Meta-Analysis. *PLoS ONE* **2016**, *11*, e0141438. [[CrossRef](#)]
106. Patel, P.; Baradaran, H.; Delgado, D.; Askin, G.; Christos, P.; John Tsiouris, A.; Gupta, A. MR perfusion-weighted imaging in the evaluation of high-grade gliomas after treatment: A systematic review and meta-analysis. *Neuro Oncol.* **2017**, *19*, 118–127. [[CrossRef](#)]
107. Tsakiris, C.; Siempis, T.; Alexiou, G.A.; Zikou, A.; Sioka, C.; Voulgaris, S.; Argyropoulou, M.I. Differentiation Between True Tumor Progression of Glioblastoma and Pseudoprogression Using Diffusion-Weighted Imaging and Perfusion-Weighted Imaging: Systematic Review and Meta-analysis. *World Neurosurg.* **2020**, *144*, e100–e109. [[CrossRef](#)]
108. Okuchi, S.; Rojas-Garcia, A.; Ulyte, A.; Lopez, I.; Ušinskienė, J.; Lewis, M.; Hassanein, S.M.; Sanverdi, E.; Golay, X.; Thust, S.; et al. Diagnostic accuracy of dynamic contrast-enhanced perfusion MRI in stratifying gliomas: A systematic review and meta-analysis. *Cancer Med.* **2019**, *8*, 5564–5573. [[CrossRef](#)]
109. Miyoshi, F.; Shinohara, Y.; Kambe, A.; Kuya, K.; Murakami, A.; Kurosaki, M.; Ogawa, T. Utility of intravoxel incoherent motion magnetic resonance imaging and arterial spin labeling for recurrent glioma after bevacizumab treatment. *Acta Radiol.* **2018**, *59*, 1372–1379. [[CrossRef](#)]
110. Nyberg, E.; Honce, J.; Kleinschmidt-DeMasters, B.K.; Shukri, B.; Kreidler, S.; Nagae, L. Arterial spin labeling: Pathologically proven superiority over conventional MRI for detection of high-grade glioma progression after treatment. *Neuroradiol. J.* **2016**, *29*, 377–383. [[CrossRef](#)]

111. Jain, R.; Narang, J.; Schultz, L.; Scarpance, L.; Saksena, S.; Brown, S.; Rock, J.P.; Rosenblum, M.; Gutierrez, J.; Mikkelsen, T. Permeability Estimates in Histopathology-Proved Treatment-Induced Necrosis Using Perfusion CT: Can These Add to Other Perfusion Parameters in Differentiating from Recurrent/Progressive Tumors? *Am. J. Neuroradiol.* **2011**, *32*, 658–663. [[CrossRef](#)]
112. Jain, R.; Scarpance, L.; Ellika, S.; Schultz, L.R.; Rock, J.P.; Rosenblum, M.L.; Patel, S.C.; Lee, T.-Y.; Mikkelsen, T. First-pass perfusion computed tomography: Initial experience in differentiating recurrent brain tumors from radiation effects and radiation necrosis. *Neurosurgery* **2007**, *61*, 778–787. [[CrossRef](#)] [[PubMed](#)]
113. Baker, S.G.; Kramer, B.S. Evaluating surrogate endpoints, prognostic markers, and predictive markers: Some simple themes. *Clin. Trials* **2015**, *12*, 299–308. [[CrossRef](#)] [[PubMed](#)]
114. Ulyte, A.; Katsaros, V.K.; Liouta, E.; Stranjalis, G.; Boskos, C.; Papanikolaou, N.; Usinskiene, J.; Bisdas, S. Prognostic value of preoperative dynamic contrast-enhanced MRI perfusion parameters for high-grade glioma patients. *Neuroradiology* **2016**, *58*, 1197–1208. [[CrossRef](#)] [[PubMed](#)]
115. Ellingson, B.M.; Yao, J.; Raymond, C.; Nathanson, D.A.; Chakhoyan, A.; Simpson, J.; Garner, J.S.; Olivero, A.G.; Mueller, L.U.; Rodon, J.; et al. Multiparametric MR-PET Imaging Predicts Pharmacokinetics and Clinical Response to GDC-0084 in Patients with Recurrent High-Grade Glioma. *Clin. Cancer Res.* **2020**, *26*, 3135–3144. [[CrossRef](#)] [[PubMed](#)]
116. White, M.L.; Zhang, Y.; Yu, F.; Shonka, N.; Aizenberg, M.R.; Adapa, P.; Kazmi, S.A.J. Post-operative perfusion and diffusion MR imaging and tumor progression in high-grade gliomas. *PLoS ONE* **2019**, *14*, e0213905. [[CrossRef](#)] [[PubMed](#)]
117. Jain, R.; Poisson, L.M.; Gutman, D.; Scarpance, L.; Hwang, S.N.; Holder, C.A.; Wintermark, M.; Rao, A.; Colen, R.R.; Kirby, J.; et al. Outcome Prediction in Patients with Glioblastoma by Using Imaging, Clinical, and Genomic Biomarkers: Focus on the Nonenhancing Component of the Tumor. *Radiology* **2014**, *272*, 484–493. [[CrossRef](#)] [[PubMed](#)]
118. Law, M.; Young, R.J.; Babb, J.S.; Peccerelli, N.; Chheang, S.; Gruber, M.L.; Miller, D.C.; Golfinos, J.G.; Zagzag, D.; Johnson, G. Gliomas: Predicting Time to Progression or Survival with Cerebral Blood Volume Measurements at Dynamic Susceptibility-weighted Contrast-enhanced Perfusion MR Imaging. *Radiology* **2008**, *247*, 490–498. [[CrossRef](#)]
119. Burth, S.; Kickingereder, P.; Eidel, O.; Tichy, D.; Bonekamp, D.; Weberling, L.; Wick, A.; Löw, S.; Hertenstein, A.; Nowosielski, M.; et al. Clinical parameters outweigh diffusion- and perfusion-derived MRI parameters in predicting survival in newly diagnosed glioblastoma. *Neuro Oncol.* **2016**, *18*, 1673–1679. [[CrossRef](#)]
120. Kim, H.S.; Kwon, S.L.; Choi, S.H.; Hwang, I.; Kim, T.M.; Park, C.-K.; Park, S.-H.; Won, J.-K.; Kim, I.H.; Lee, S.T. Prognostication of anaplastic astrocytoma patients: Application of contrast leakage information of dynamic susceptibility contrast-enhanced MRI and dynamic contrast-enhanced MRI. *Eur. Radiol.* **2020**, *30*, 2171–2181. [[CrossRef](#)]
121. Stecco, A.; Amatuzo, P.; Sponghini, A.P.; Platini, F.; Quagliozzi, M.; Buemi, F.; Guenzi, E.; Carriero, A. Prognostic value of relative cerebral blood volume in patients with recurrent glioblastoma multiforme treated with bevacizumab. *J. Neurosurg. Sci.* **2019**, *63*, 394–401. [[CrossRef](#)]
122. Lucas, J.T., Jr.; Knapp, B.J.; Uh, J.; Hua, C.-H.; Merchant, T.E.; Hwang, S.N.; Patay, Z.; Broniscer, A. Posttreatment DSC-MRI is Predictive of Early Treatment Failure in Children with Supratentorial High-Grade Glioma Treated with Erlotinib. *Clin. Neuroradiol.* **2018**, *28*, 393–400. [[CrossRef](#)] [[PubMed](#)]
123. McCullough, B.J.; Ader, V.; Aguedan, B.; Feng, X.; Susanto, D.; Benkers, T.L.; Henson, J.W.; Mayberg, M.; Cobbs, C.S.; Gwinn, R.P.; et al. Preoperative relative cerebral blood volume analysis in gliomas predicts survival and mitigates risk of biopsy sampling error. *J. Neurooncol.* **2018**, *136*, 181–188. [[CrossRef](#)] [[PubMed](#)]
124. Sanz-Requena, R.; Revert-Ventura, A.J.; García-Martí, G.; Salamé-Gamarra, F.; Pérez-Girbés, A.; Mollá-Olmos, E.; Martí-Bonmatí, L. Post-treatment changes of tumour perfusion parameters can help to predict survival in patients with high-grade astrocytoma. *Eur. Radiol.* **2017**, *27*, 3392–3400. [[CrossRef](#)] [[PubMed](#)]
125. Vajapeyam, S.; Brown, D.; Billups, C.; Patay, Z.; Vezina, G.; Shiroishi, M.S.; Law, M.; Baxter, P.; Onar-Thomas, A.; Fangusaro, J.R.; et al. Advanced ADC Histogram, Perfusion, and Permeability Metrics Show an Association with Survival and Pseudoprogression in Newly Diagnosed Diffuse Intrinsic Pontine Glioma: A Report from the Pediatric Brain Tumor Consortium. *Am. J. Neuroradiol.* **2020**, *41*, 718–724. [[CrossRef](#)]
126. Spampinato, M.V.; Schiarella, C.; Cianfoni, A.; Giglio, P.; Welsh, C.T.; Bisdas, S.; Rumboldt, Z. Correlation between Cerebral Blood Volume Measurements by Perfusion-Weighted Magnetic Resonance Imaging and Two-Year Progression-Free Survival in Gliomas. *Neuroradiol. J.* **2013**, *26*, 385–395. [[CrossRef](#)]
127. Mangla, R.; Ginat, D.T.; Kamalian, S.; Milano, M.T.; Korones, D.N.; Walter, K.A.; Ekholm, S. Correlation between progression free survival and dynamic susceptibility contrast MRI perfusion in WHO grade III glioma subtypes. *J. Neurooncol.* **2014**, *116*, 325–331. [[CrossRef](#)]
128. Bonekamp, D.; Mouridsen, K.; Radbruch, A.; Kurz, F.T.; Eidel, O.; Wick, A.; Schlemmer, H.-P.; Wick, W.; Bendszus, M.; Østergaard, L.; et al. Assessment of tumor oxygenation and its impact on treatment response in bevacizumab-treated recurrent glioblastoma. *J. Cereb. Blood Flow Metab.* **2017**, *37*, 485–494. [[CrossRef](#)]
129. Jain, R.; Poisson, L.; Narang, J.; Gutman, D.; Scarpance, L.; Hwang, S.N.; Holder, C.; Wintermark, M.; Colen, R.R.; Kirby, J.; et al. Genomic Mapping and Survival Prediction in Glioblastoma: Molecular Subclassification Strengthened by Hemodynamic Imaging Biomarkers. *Radiology* **2013**, *267*, 212–220. [[CrossRef](#)]
130. Jenkinson, M.D.; Smith, T.S.; Joyce, K.A.; Fildes, D.; Broome, J.; du Plessis, D.G.; Haylock, B.; Husband, D.J.; Warnke, P.C.; Walker, C. Cerebral blood volume, genotype and chemosensitivity in oligodendroglial tumours. *Neuroradiology* **2006**, *48*, 703–713. [[CrossRef](#)]

131. Jabehdar Maralani, P.; Melhem, E.R.; Wang, S.; Herskovits, E.H.; Voluck, M.R.; Kim, S.J.; Learned, K.O.; O'Rourke, D.M.; Mohan, S. Association of dynamic susceptibility contrast enhanced MR Perfusion parameters with prognosis in elderly patients with glioblastomas. *Eur. Radiol.* **2015**, *25*, 2738–2744. [[CrossRef](#)]
132. Çoban, G.; Mohan, S.; Kural, F.; Wang, S.; O'Rourke, D.M.; Poptani, H. Prognostic Value of Dynamic Susceptibility Contrast-Enhanced and Diffusion-Weighted MR Imaging in Patients with Glioblastomas. *Am. J. Neuroradiol.* **2015**, *36*, 1247–1252. [[CrossRef](#)] [[PubMed](#)]
133. Fong, C.; Parpia, S.; Yemen, B.; Tsai, S.; Greenspoon, J. Using Magnetic Resonance Perfusion to Stratify Overall Survival in Treated High-Grade Gliomas. *Can. J. Neurol. Sci.* **2019**, *46*, 533–539. [[CrossRef](#)] [[PubMed](#)]
134. Juan-Albarracín, J.; Fuster-García, E.; Pérez-Girbés, A.; Aparici-Robles, F.; Alberich-Bayarri, Á.; Revert-Ventura, A.; Martí-Bonmatí, L.; García-Gómez, J.M. Glioblastoma: Vascular Habitats Detected at Preoperative Dynamic Susceptibility-weighted Contrast-enhanced Perfusion MR Imaging Predict Survival. *Radiology* **2018**, *287*, 944–954. [[CrossRef](#)] [[PubMed](#)]
135. Cao, Y.; Tsien, C.I.; Nagesh, V.; Junck, L.; Ten Haken, R.; Ross, B.D.; Chenevert, T.L.; Lawrence, T.S. Clinical investigation survival prediction in high-grade gliomas by MRI perfusion before and during early stage of RT. *Int. J. Radiat. Oncol. Biol. Phys.* **2006**, *64*, 876–885. [[CrossRef](#)] [[PubMed](#)]
136. Bag, A.K.; Cezayirli, P.C.; Davenport, J.J.; Gaddikeri, S.; Fathallah-Shaykh, H.M.; Cantor, A.; Han, X.S.; Nabors, L.B. Survival analysis in patients with newly diagnosed primary glioblastoma multiforme using pre- and post-treatment peritumoral perfusion imaging parameters. *J. Neurooncol.* **2014**, *120*, 361–370. [[CrossRef](#)] [[PubMed](#)]
137. Danchavijitr, N.; Waldman, A.D.; Tozer, D.J.; Benton, C.E.; Brasil Caseiras, G.; Tofts, P.S.; Rees, J.H.; Jäger, H.R. Low-Grade Gliomas: Do Changes in rCBV Measurements at Longitudinal Perfusion-weighted MR Imaging Predict Malignant Transformation? *Radiology* **2008**, *247*, 170–178. [[CrossRef](#)] [[PubMed](#)]
138. Schmainda, K.M.; Zhang, Z.; Prah, M.; Snyder, B.S.; Gilbert, M.R.; Sorensen, A.G.; Barboriak, D.P.; Boxerman, J.L. Dynamic susceptibility contrast MRI measures of relative cerebral blood volume as a prognostic marker for overall survival in recurrent glioblastoma: Results from the ACRIN 6677/RTOG 0625 multicenter trial. *Neuro Oncol.* **2015**, *17*, 1148–1156. [[CrossRef](#)]
139. Schmainda, K.M.; Prah, M.A.; Marques, H.; Kim, E.; Barboriak, D.P.; Boxerman, J.L. Value of dynamic contrast perfusion MRI to predict early response to bevacizumab in newly diagnosed glioblastoma: Results from ACRIN 6686 multicenter trial. *Neuro Oncol.* **2021**, *23*, 314–323. [[CrossRef](#)]
140. Kang, Y.; Hong, E.K.; Rhim, J.H.; Yoo, R.-E.; Kang, K.M.; Yun, T.J.; Kim, J.-H.; Sohn, C.-H.; Park, S.-W.; Choi, S.H. Prognostic Value of Dynamic Contrast-Enhanced MRI-Derived Pharmacokinetic Variables in Glioblastoma Patients: Analysis of Contrast-Enhancing Lesions and Non-Enhancing T2 High-Signal Intensity Lesions. *Korean J. Radiol.* **2020**, *21*, 707–716. [[CrossRef](#)]
141. Hwang, I.; Choi, S.H.; Park, C.-K.; Kim, T.M.; Park, S.-H.; Won, J.K.; Kim, I.H.; Lee, S.-T.; Yoo, R.-E.; Kang, K.M.; et al. Dynamic Contrast-Enhanced MR Imaging of Nonenhancing T2 High-Signal-Intensity Lesions in Baseline and Posttreatment Glioblastoma: Temporal Change and Prognostic Value. *Am. J. Neuroradiol.* **2020**, *41*, 49–56. [[CrossRef](#)]
142. Ly, K.I.; Vakulenko-Lagun, B.; Emblem, K.E.; Ou, Y.; Da, X.; Betensky, R.A.; Kalpathy-Cramer, J.; Duda, D.G.; Jain, R.K.; Chi, A.S.; et al. Probing tumor microenvironment in patients with newly diagnosed glioblastoma during chemoradiation and adjuvant temozolomide with functional MRI. *Sci. Rep.* **2018**, *8*, 17062. [[CrossRef](#)] [[PubMed](#)]
143. Hilario, A.; Hernandez-Lain, A.; Sepulveda, J.M.; Lagares, A.; Perez-Nuñez, A.; Ramos, A. Perfusion MRI grading diffuse gliomas: Impact of permeability parameters on molecular biomarkers and survival. *Neurocirugía* **2019**, *30*, 11–18. [[CrossRef](#)] [[PubMed](#)]
144. Mills, S.J.; Patankar, T.A.; Haroon, H.A.; Balériaux, D.; Swindell, R.; Jackson, A. Do Cerebral Blood Volume and Contrast Transfer Coefficient Predict Prognosis in Human Glioma? *Am. J. Neuroradiol.* **2006**, *27*, 853–858. [[PubMed](#)]
145. Nguyen, T.B.; Cron, G.O.; Mercier, J.F.; Foottit, C.; Torres, C.H.; Chakraborty, S.; Woulfe, J.; Jansen, G.H.; Caudrelier, J.M.; Sinclair, J.; et al. Preoperative Prognostic Value of Dynamic Contrast-Enhanced MRI-Derived Contrast Transfer Coefficient and Plasma Volume in Patients with Cerebral Gliomas. *Am. J. Neuroradiol.* **2015**, *36*, 63–69. [[CrossRef](#)]
146. Bonekamp, D.; Deike, K.; Wiestler, B.; Wick, W.; Bendszus, M.; Radbruch, A.; Heiland, S. Association of overall survival in patients with newly diagnosed glioblastoma with contrast-enhanced perfusion MRI: Comparison of intraindividually matched T1- and T2*-based bolus techniques. *J. Magn. Reson. Imaging* **2015**, *42*, 87–96. [[CrossRef](#)]
147. Kickingereder, P.; Wiestler, B.; Burth, S.; Wick, A.; Nowosielski, M.; Heiland, S.; Schlemmer, H.-P.; Wick, W.; Bendszus, M.; Radbruch, A. Relative cerebral blood volume is a potential predictive imaging biomarker of bevacizumab efficacy in recurrent glioblastoma. *Neuro Oncol.* **2015**, *17*, 1139–1147. [[CrossRef](#)]
148. Larsson, C.; Groote, I.; Vardal, J.; Kleppstø, M.; Odland, A.; Brandal, P.; Due-Tønnessen, P.; Holme, S.S.; Hope, T.R.; Meling, T.R.; et al. Prediction of survival and progression in glioblastoma patients using temporal perfusion changes during radiochemotherapy. *Magn. Reson. Imaging* **2020**, *68*, 106–112. [[CrossRef](#)]
149. Bisdas, S.; Smrdel, U.; Bajrovic, F.F.; Surlan-Popovic, K. Assessment of Progression-Free-Survival in Glioblastomas by Intratreatment Dynamic Contrast-Enhanced MRI. *Clin. Neuroradiol.* **2016**, *26*, 39–45. [[CrossRef](#)]
150. O'Neill, A.F.; Qin, L.; Wen, P.Y.; de Groot, J.F.; Van den Abbeele, A.D.; Yap, J.T. Demonstration of DCE-MRI as an early pharmacodynamic biomarker of response to VEGF Trap in glioblastoma. *J. Neurooncol.* **2016**, *130*, 495–503. [[CrossRef](#)]
151. Møller, S.; Lundemann, M.; Law, I.; Poulsen, H.S.; Larsson, H.B.W.; Engelholm, S.A. Early changes in perfusion of glioblastoma during radio- and chemotherapy evaluated by T1-dynamic contrast enhanced magnetic resonance imaging. *Acta Oncol.* **2015**, *54*, 1521–1528. [[CrossRef](#)]

152. Park, Y.W.; Ahn, S.S.; Moon, J.H.; Kim, E.H.; Kang, S.-G.; Chang, J.H.; Kim, S.H.; Lee, S.-K. Dynamic contrast-enhanced MRI may be helpful to predict response and prognosis after bevacizumab treatment in patients with recurrent high-grade glioma: Comparison with diffusion tensor and dynamic susceptibility contrast imaging. *Neuroradiology* **2021**, *63*, 1811–1822. [CrossRef]
153. Choi, Y.S.; Ahn, S.S.; Lee, H.-J.; Chang, J.H.; Kang, S.-G.; Kim, E.H.; Kim, S.H.; Lee, S.-K. The Initial Area Under the Curve Derived from Dynamic Contrast-Enhanced MRI Improves Prognosis Prediction in Glioblastoma with Unmethylated MGMT Promoter. *Am. J. Neuroradiol.* **2017**, *38*, 1528–1535. [CrossRef] [PubMed]
154. Choi, S.H.; Jung, S.C.; Kim, K.W.; Lee, J.Y.; Choi, Y.; Park, S.H.; Kim, H.S. Perfusion MRI as the predictive/prognostic and pharmacodynamic biomarkers in recurrent malignant glioma treated with bevacizumab: A systematic review and a time-to-event meta-analysis. *J. Neurooncol.* **2016**, *128*, 185–194. [CrossRef] [PubMed]
155. Furtner, J.; Bender, B.; Braun, C.; Schittenhelm, J.; Skardelly, M.; Ernemann, U.; Bisdas, S. Prognostic Value of Blood Flow Measurements Using Arterial Spin Labeling in Gliomas. *PLoS ONE* **2014**, *9*, e99616. [CrossRef]
156. Jain, R.; Narang, J.; Griffith, B.; Bagher-Ebadian, H.; Scarpace, L.; Mikkelsen, T.; Littenberg, B.; Schultz, L.R. Prognostic vascular imaging biomarkers in high-grade gliomas: Tumor permeability as an adjunct to blood volume estimates. *Acad Radiol.* **2013**, *20*, 478–485. [CrossRef] [PubMed]
157. Jain, R.; Griffith, B.; Alotaibi, F.; Zagzag, D.; Fine, H.; Golfinos, J.; Schultz, L. Glioma Angiogenesis and Perfusion Imaging: Understanding the Relationship between Tumor Blood Volume and Leakiness with Increasing Glioma Grade. *Am. J. Neuroradiol.* **2015**, *36*, 2030–2035. [CrossRef]
158. Yeung, T.P.C.; Wang, Y.; He, W.; Urbini, B.; Gafà, R.; Ulazzi, L.; Yartsev, S.; Bauman, G.; Lee, T.-Y.; Fainardi, E.; et al. Survival prediction in high-grade gliomas using CT perfusion imaging. *J. Neuro Oncol.* **2015**, *123*, 93–102. [CrossRef]
159. Stadlbauer, A.; Kinfe, T.M.; Eyüpoglu, I.; Zimmermann, M.; Kitzwögerer, M.; Podar, K.; Buchfelder, M.; Heinz, G.; Oberndorfer, S.; Marhold, F. Tissue Hypoxia and Alterations in Microvascular Architecture Predict Glioblastoma Recurrence in Humans. *Clin. Cancer Res.* **2020**. [CrossRef]
160. Stadlbauer, A.; Zimmermann, M.; Doerfler, A.; Oberndorfer, S.; Buchfelder, M.; Coras, R.; Kitzwögerer, M.; Roessler, K. Intratumoral heterogeneity of oxygen metabolism and neovascularization uncovers 2 survival-relevant subgroups of IDH1 wild-type glioblastoma. *Neuro Oncol.* **2018**, *20*, 1536–1546. [CrossRef]
161. Stadlbauer, A.; Eyüpoglu, I.; Buchfelder, M.; Dörfler, A.; Zimmermann, M.; Heinz, G.; Oberndorfer, S. Vascular architecture mapping for early detection of glioblastoma recurrence. *Neurosurg. Focus.* **2019**, *47*, E14. [CrossRef]
162. Fuster-Garcia, E.; Juan-Albarracín, J.; García-Ferrando, G.A.; Martí-Bonmatí, L.; Aparici-Robles, F.; García-Gómez, J.M. Improving the estimation of prognosis for glioblastoma patients by MR based hemodynamic tissue signatures. *NMR Biomed.* **2018**, *31*, e4006. [CrossRef] [PubMed]
163. Álvarez-Torres, M.D.M.; Juan-Albarracín, J.; Fuster-Garcia, E.; Bellvís-Bataller, F.; Lorente, D.; Reynés, G.; de Mora, J.F.; Aparici-Robles, F.; Botella, C.; Muñoz-Langa, J.; et al. Robust association between vascular habitats and patient prognosis in glioblastoma: An international multicenter study. *J. Magn. Reson. Imaging* **2020**, *51*, 1478–1486. [CrossRef] [PubMed]
164. Chelebian, E.; Fuster-Garcia, E.; Álvarez-Torres, M.D.M.; Juan-Albarracín, J.; García-Gómez, J.M. Higher vascularity at infiltrated peripheral edema differentiates proneural glioblastoma subtype. *PLoS ONE* **2020**, *15*, e0232500. [CrossRef] [PubMed]
165. Álvarez-Torres, M.D.M.; Fuster-García, E.; Balaña, C.; Puig, J.; García-Gómez, J.M. Lack of Benefit of Extending Temozolomide Treatment in Patients with High Vascular Glioblastoma with Methylated MGMT. *Cancers* **2021**, *13*, 5420. [CrossRef]
166. Prada, F.; Vetrano, I.G.; Gennari, A.G.; Mauri, G.; Martegani, A.; Solbiati, L.; Sconfienza, L.M.; Quaia, E.; Kearns, K.N.; Kalani, M.Y.S.; et al. How to Perform Intra-Operative Contrast-Enhanced Ultrasound of the Brain—A WFUMB Position Paper. *Ultrasound Med. Biol.* **2021**, *47*, 2006–2016. [CrossRef]
167. Prada, F.; Vitale, V.; Del Bene, M.; Boffano, C.; Sconfienza, L.M.; Pinzi, V.; Mauri, G.; Solbiati, L.; Sakas, G.; Kolev, V.; et al. Contrast-enhanced MR Imaging versus Contrast-enhanced US: A Comparison in Glioblastoma Surgery by Using Intraoperative Fusion Imaging. *Radiology* **2017**, *285*, 242–249. [CrossRef]
168. Della Pepa, G.M.; Menna, G.; Ius, T.; Di Bonaventura, R.; Altieri, R.; Marchese, E.; Olivi, A.; Sabatino, G.; La Rocca, G. Contrast enhanced ultrasound (CEUS) applications in neurosurgical and neurological settings—New scenarios for brain and spinal cord ultrasonography. A systematic review. *Clin. Neurol. Neurosurg.* **2020**, *198*, 106105. [CrossRef]
169. Kearns, K.N.; Sokolowski, J.D.; Chadwell, K.; Chandler, M.; Kiernan, T.; Prada, F.; Kalani, M.Y.S.; Park, M.S. The role of contrast-enhanced ultrasound in neurosurgical disease. *Neurosurg. Focus* **2019**, *47*, E8. [CrossRef]
170. Wang, J.; Yang, Y.; Liu, X.; Duan, Y. Intraoperative contrast-enhanced ultrasound for cerebral glioma resection and the relationship between microvascular perfusion and microvessel density. *Clin. Neurol. Neurosurg.* **2019**, *186*, 105512. [CrossRef]
171. Cheng, L.-G.; He, W.; Zhang, H.-X.; Song, Q.; Ning, B.; Li, H.-Z.; He, Y.; Lin, S. Intraoperative Contrast Enhanced Ultrasound Evaluates the Grade of Glioma. Available online: <https://www.hindawi.com/journals/bmri/2016/2643862/> (accessed on 7 December 2021).
172. Prada, F.; Mattei, L.; Del Bene, M.; Aiani, L.; Saini, M.; Casali, C.; Filippini, A.; Legnani, F.G.; Perin, A.; Saladino, A.; et al. Intraoperative Cerebral Glioma Characterization with Contrast Enhanced Ultrasound. *BioMed Res. Int.* **2014**, *2014*, e484261. [CrossRef]
173. Berhouma, M.; Picart, T.; Dumot, C.; Pelissou-Guyotat, I.; Meyronet, D.; Ducray, F.; Honnorat, J.; Eker, O.; Guyotat, J.; Lukaszewicz, A.-C.; et al. Alterations of cerebral microcirculation in peritumoral edema: Feasibility of in vivo sidestream dark-field imaging in intracranial meningiomas. *Neuro Oncol. Adv.* **2020**, *2*, vdaa108. [CrossRef] [PubMed]

174. Tahhan, N.; Balanca, B.; Fierstra, J.; Waelchli, T.; Picart, T.; Dumot, C.; Eker, O.; Marinesco, S.; Radovanovic, I.; Cotton, F.; et al. Intraoperative cerebral blood flow monitoring in neurosurgery: A review of contemporary technologies and emerging perspectives. *Neurochirurgie* **2021**. *online ahead of print*. [[CrossRef](#)] [[PubMed](#)]
175. Le Bihan, D.; Breton, E.; Lallemand, D.; Grenier, P.; Cabanis, E.; Laval-Jeantet, M. MR imaging of intravoxel incoherent motions: Application to diffusion and perfusion in neurologic disorders. *Radiology* **1986**, *161*, 401–407. [[CrossRef](#)]
176. Le Bihan, D.; Breton, E.; Lallemand, D.; Aubin, M.L.; Vignaud, J.; Laval-Jeantet, M. Separation of diffusion and perfusion in intravoxel incoherent motion MR imaging. *Radiology* **1988**, *168*, 497–505. [[CrossRef](#)] [[PubMed](#)]
177. Federau, C. Measuring Perfusion: Intravoxel Incoherent Motion MR Imaging. *Magn. Reson. Imaging Clin. N. Am.* **2021**, *29*, 233–242. [[CrossRef](#)]
178. Suh, C.H.; Kim, H.S.; Lee, S.S.; Kim, N.; Yoon, H.M.; Choi, C.-G.; Kim, S.J. Atypical Imaging Features of Primary Central Nervous System Lymphoma That Mimics Glioblastoma: Utility of Intravoxel Incoherent Motion MR Imaging. *Radiology* **2014**, *272*, 504–513. [[CrossRef](#)]
179. Yamashita, K.; Hiwatashi, A.; Togao, O.; Kikuchi, K.; Kitamura, Y.; Mizoguchi, M.; Yoshimoto, K.; Kuga, D.; Suzuki, S.O.; Baba, S.; et al. Diagnostic utility of intravoxel incoherent motion mr imaging in differentiating primary central nervous system lymphoma from glioblastoma multiforme. *J. Magn. Reson. Imaging* **2016**, *44*, 1256–1261. [[CrossRef](#)]
180. Keil, V.C.; Mädler, B.; Gielen, G.H.; Pintea, B.; Hiththetiya, K.; Gaspranova, A.R.; Gieseke, J.; Simon, M.; Schild, H.H.; Hadizadeh, D.R. Intravoxel incoherent motion MRI in the brain: Impact of the fitting model on perfusion fraction and lesion differentiability. *J. Magn. Reson. Imaging* **2017**, *46*, 1187–1199. [[CrossRef](#)]
181. Wang, X.; Chen, X.-Z.; Shi, L.; Dai, J.-P. Glioma grading and IDH1 mutational status: Assessment by intravoxel incoherent motion MRI. *Clin. Radiol.* **2019**, *74*, 651.e7–651.e14. [[CrossRef](#)]
182. Wang, C.; Dong, H. Ki-67 labeling index and the grading of cerebral gliomas by using intravoxel incoherent motion diffusion-weighted imaging and three-dimensional arterial spin labeling magnetic resonance imaging. *Acta Radiol.* **2020**, *61*, 1057–1063. [[CrossRef](#)]
183. Hu, Y.-C.; Yan, L.-F.; Wu, L.; Du, P.; Chen, B.-Y.; Wang, L.; Wang, S.-M.; Han, Y.; Tian, Q.; Yu, Y.; et al. Intravoxel incoherent motion diffusion-weighted MR imaging of gliomas: Efficacy in preoperative grading. *Sci. Rep.* **2014**, *4*, 7208. [[CrossRef](#)] [[PubMed](#)]
184. Li, W.; Niu, C.; Shakir, T.M.; Chen, T.; Zhang, M.; Wang, Z. An evidence-based approach to assess the accuracy of intravoxel incoherent motion imaging for the grading of brain tumors. *Medicine* **2018**, *97*, e13217. [[CrossRef](#)] [[PubMed](#)]
185. Jabehdar Maralani, P.; Myrehaug, S.; Mehrabian, H.; Chan, A.K.M.; Wintermark, M.; Heyn, C.; Conklin, J.; Ellingson, B.M.; Rahimi, S.; Lau, A.Z.; et al. Intravoxel incoherent motion (IVIM) modeling of diffusion MRI during chemoradiation predicts therapeutic response in IDH wildtype glioblastoma. *Radiother. Oncol.* **2021**, *156*, 258–265. [[CrossRef](#)]
186. Liu, Z.-C.; Yan, L.-F.; Hu, Y.-C.; Sun, Y.-Z.; Tian, Q.; Nan, H.-Y.; Yu, Y.; Sun, Q.; Wang, W.; Cui, G.-B. Combination of IVIM-DWI and 3D-ASL for differentiating true progression from pseudoprogression of Glioblastoma multiforme after concurrent chemoradiotherapy: Study protocol of a prospective diagnostic trial. *BMC Med. Imaging* **2017**, *17*, 10. [[CrossRef](#)] [[PubMed](#)]
187. Li, B.; Xu, D.; Zhou, J.; Wang, S.-C.; Cai, Y.-X.; Li, H.; Xu, H.-B. Monitoring Bevacizumab-Induced Tumor Vascular Normalization by Intravoxel Incoherent Motion Diffusion-Weighted MRI. *J. Magn. Reson. Imaging* **2021**. [[CrossRef](#)] [[PubMed](#)]
188. Puig, J.; Sánchez-González, J.; Blasco, G.; Daunis-i-Estadella, P.; Federau, C.; Alberich-Bayarri, Á.; Biarnes, C.; Nael, K.; Essig, M.; Jain, R.; et al. Intravoxel Incoherent Motion Metrics as Potential Biomarkers for Survival in Glioblastoma. *PLoS ONE* **2016**, *11*, e0158887. [[CrossRef](#)] [[PubMed](#)]
189. Federau, C.; Cerny, M.; Roux, M.; Mosimann, P.J.; Maeder, P.; Meuli, R.; Wintermark, M. IVIM perfusion fraction is prognostic for survival in brain glioma. *Clin. Neuroradiol.* **2017**, *27*, 485–492. [[CrossRef](#)]
190. Zhu, L.; Wu, J.; Zhang, H.; Niu, H.; Wang, L. The value of intravoxel incoherent motion imaging in predicting the survival of patients with astrocytoma. *Acta Radiol.* **2021**, *62*, 423–429. [[CrossRef](#)]
191. Hsu, Y.-Y.; Chang, C.-N.; Jung, S.-M.; Lim, K.-E.; Huang, J.-C.; Fang, S.-Y.; Liu, H.-L. Blood oxygenation level-dependent MRI of cerebral gliomas during breath holding. *J. Magn. Reson. Imaging* **2004**, *19*, 160–167. [[CrossRef](#)]
192. Iranmahboob, A.; Peck, K.K.; Brennan, N.P.; Karimi, S.; Fiscaro, R.; Hou, B.; Holodny, A.I. Vascular Reactivity Maps in Patients with Gliomas Using Breath-Holding BOLD fMRI. *J. Neuroimaging* **2016**, *26*, 232–239. [[CrossRef](#)]
193. Agarwal, S.; Sair, H.I.; Pillai, J.J. The Problem of Neurovascular Uncoupling. *Neuroimaging Clin. North. Am.* **2021**, *31*, 53–67. [[CrossRef](#)] [[PubMed](#)]
194. Slessarev, M.; Han, J.; Mardimae, A.; Prisman, E.; Preiss, D.; Volgyesi, G.; Ansel, C.; Duffin, J.; Fisher, J.A. Prospective targeting and control of end-tidal CO₂ and O₂ concentrations. *J. Physiol.* **2007**, *581*, 1207–1219. [[CrossRef](#)]
195. Fisher, J.A.; Mikulis, D.J. Cerebrovascular Reactivity: Purpose, Optimizing Methods, and Limitations to Interpretation—A Personal 20-Year Odyssey of (Re)searching. *Front. Physiol.* **2021**, *12*. [[CrossRef](#)] [[PubMed](#)]
196. Fierstra, J.; van Niftrik, B.; Piccirelli, M.; Burkhardt, J.K.; Pangalu, A.; Kocian, R.; Valavanis, A.; Weller, M.; Regli, L.; Bozinov, O. Altered intraoperative cerebrovascular reactivity in brain areas of high-grade glioma recurrence. *Magn. Reson. Imaging* **2016**, *34*, 803–808. [[CrossRef](#)] [[PubMed](#)]
197. Muscas, G.; van Niftrik, C.H.B.; Sebök, M.; Seystahl, K.; Piccirelli, M.; Stippich, C.; Weller, M.; Regli, L.; Fierstra, J. Hemodynamic investigation of peritumoral impaired blood oxygenation-level dependent cerebrovascular reactivity in patients with diffuse glioma. *Magn. Reson. Imaging* **2020**, *70*, 50–56. [[CrossRef](#)]

198. Sebök, M.; van Niftrik, C.H.B.; Muscas, G.; Pangalu, A.; Seystahl, K.; Weller, M.; Regli, L.; Fierstra, J. Hypermetabolism and impaired cerebrovascular reactivity beyond the standard MRI-identified tumor border indicate diffuse glioma extended tissue infiltration. *Neuro Oncol. Adv.* **2021**, *3*, vdab048. [[CrossRef](#)] [[PubMed](#)]
199. Fierstra, J.; van Niftrik, C.; Piccirelli, M.; Bozinov, O.; Pangalu, A.; Krayenbühl, N.; Valavanis, A.; Weller, M.; Regli, L. Diffuse gliomas exhibit whole brain impaired cerebrovascular reactivity. *Magn. Reson. Imaging* **2018**, *45*, 78–83. [[CrossRef](#)]
200. Sebök, M.; van Niftrik, C.H.B.; Halter, M.; Hiller, A.; Seystahl, K.; Pangalu, A.; Weller, M.; Stippich, C.; Regli, L.; Fierstra, J. Crossed Cerebellar Diaschisis in Patients with Diffuse Glioma Is Associated with Impaired Supratentorial Cerebrovascular Reactivity and Worse Clinical Outcome. *Cerebellum* **2020**, *19*, 824–832. [[CrossRef](#)]
201. Bashat, D.B.; Artzi, M.; Ami, H.B.; Aizenstein, O.; Blumenthal, D.T.; Bokstein, F.; Corn, B.W.; Ram, Z.; Kanner, A.A.; Lifschitz-Mercer, B.; et al. Hemodynamic Response Imaging: A Potential Tool for the Assessment of Angiogenesis in Brain Tumors. *PLoS ONE* **2012**, *7*, e49416. [[CrossRef](#)]
202. Poublanc, J.; Sobczyk, O.; Shafi, R.; Sayin, E.S.; Schulman, J.; Duffin, J.; Uludag, K.; Wood, J.C.; Vu, C.; Dharmakumar, R.; et al. Perfusion MRI using endogenous deoxyhemoglobin as a contrast agent: Preliminary data. *Magn. Reson. Med.* **2021**, *86*, 3012–3021. [[CrossRef](#)]
203. Vu, C.; Chai, Y.; Coloigner, J.; Nederveen, A.J.; Borzage, M.; Bush, A.; Wood, J.C. Quantitative perfusion mapping with induced transient hypoxia using BOLD MRI. *Magn. Reson. Med.* **2021**, *85*, 168–181. [[CrossRef](#)]
204. Sayin, E.S.; Schulman, J.; Poublanc, J.; Levine, H.; Venkatraghavan, L.; Uludag, K.; Duffin, J.; Fisher, J.A.; Mikulis, D.J.; Sobczyk, O. Cerebral perfusion imaging: Hypoxia-induced deoxyhemoglobin or gadolinium? *bioRxiv* **2021**. [[CrossRef](#)]
205. Kiviniemi, A.; Gardberg, M.; Ek, P.; Frantzén, J.; Bobacka, J.; Minn, H. Gadolinium retention in gliomas and adjacent normal brain tissue: Association with tumor contrast enhancement and linear/macrocyclic agents. *Neuroradiology* **2019**, *61*, 535–544. [[CrossRef](#)]
206. Stumpo, V.; Sebök, M.; van Niftrik, C.H.B.; Seystahl, K.; Hainc, N.; Kulcsar, Z.; Weller, M.; Regli, L.; Fierstra, J. Feasibility of glioblastoma tissue response mapping with physiologic BOLD imaging using precise oxygen and carbon dioxide challenge. *Magn. Reson. Mater. Phy.* **2021**. *online ahead of print*. [[CrossRef](#)] [[PubMed](#)]
207. Stumpo, V.; Kernbach, J.M.; van Niftrik, C.H.B.; Sebök, M.; Fierstra, J.; Regli, L.; Serra, C.; Staartjes, V.E. Machine Learning Algorithms in Neuroimaging: An Overview. *Acta Neurochir. Suppl.* **2022**, *134*, 125–138. [[CrossRef](#)] [[PubMed](#)]
208. Lambin, P.; Leijenaar, R.T.H.; Deist, T.M.; Peerlings, J.; de Jong, E.E.C.; van Timmeren, J.; Sanduleanu, S.; Larue, R.T.H.M.; Even, A.J.G.; Jochems, A.; et al. Radiomics: The bridge between medical imaging and personalized medicine. *Nat. Rev. Clin. Oncol.* **2017**, *14*, 749–762. [[CrossRef](#)]
209. Staartjes, V.E.; Stumpo, V.; Kernbach, J.M.; Klukowska, A.M.; Gadraj, P.S.; Schröder, M.L.; Veeravagu, A.; Stienen, M.N.; van Niftrik, C.H.B.; Serra, C.; et al. Machine learning in neurosurgery: A global survey. *Acta Neurochir.* **2020**, *162*, 3081–3091. [[CrossRef](#)]
210. Wagner, M.W.; Namdar, K.; Biswas, A.; Monah, S.; Khalvati, F.; Ertl-Wagner, B.B. Radiomics, machine learning, and artificial intelligence—what the neuroradiologist needs to know. *Neuroradiology* **2021**, *63*, 1957–1967. [[CrossRef](#)]
211. Park, C.J.; Han, K.; Kim, H.; Ahn, S.S.; Choi, D.; Park, Y.W.; Chang, J.H.; Kim, S.H.; Cha, S.; Lee, S.-K. MRI Features May Predict Molecular Features of Glioblastoma in Isocitrate Dehydrogenase Wild-Type Lower-Grade Gliomas. *Am. J. Neuroradiol.* **2021**, *42*, 448–456. [[CrossRef](#)]
212. Gusev, Y.; Bhuvaneshwar, K.; Song, L.; Zenklusen, J.-C.; Fine, H.; Madhavan, S. The rembrandt study, a large collection of genomic data from brain cancer patients. *Sci. Data* **2018**, *5*, 180158. [[CrossRef](#)]
213. Sudre, C.H.; Panovska-Griffiths, J.; Sanverdi, E.; Brandner, S.; Katsaros, V.K.; Stranjalis, G.; Pizzini, F.B.; Ghimenton, C.; Surlan-Popovic, K.; Avsenik, J.; et al. Machine learning assisted DSC-MRI radiomics as a tool for glioma classification by grade and mutation status. *BMC Med. Inform. Decis. Mak.* **2020**, *20*, 149. [[CrossRef](#)] [[PubMed](#)]
214. Pak, E.; Choi, K.S.; Choi, S.H.; Park, C.-K.; Kim, T.M.; Park, S.-H.; Lee, J.H.; Lee, S.-T.; Hwang, I.; Yoo, R.-E.; et al. Prediction of Prognosis in Glioblastoma Using Radiomics Features of Dynamic Contrast-Enhanced MRI. *Korean J. Radiol.* **2021**, *22*, 1514–1524. [[CrossRef](#)] [[PubMed](#)]
215. Hashido, T.; Saito, S.; Ishida, T. A radiomics-based comparative study on arterial spin labeling and dynamic susceptibility contrast perfusion-weighted imaging in gliomas. *Sci. Rep.* **2020**, *10*, 6121. [[CrossRef](#)] [[PubMed](#)]
216. Manikis, G.C.; Ioannidis, G.S.; Siakallis, L.; Nikiforaki, K.; Iv, M.; Vozlic, D.; Surlan-Popovic, K.; Wintermark, M.; Bisdas, S.; Marias, K. Multicenter DSC-MRI-Based Radiomics Predict IDH Mutation in Gliomas. *Cancers* **2021**, *13*, 3965. [[CrossRef](#)]
217. Peng, H.; Huo, J.; Li, B.; Cui, Y.; Zhang, H.; Zhang, L.; Ma, L. Predicting Isocitrate Dehydrogenase (IDH) Mutation Status in Gliomas Using Multiparameter MRI Radiomics Features. *J. Magn. Reson. Imaging* **2021**, *53*, 1399–1407. [[CrossRef](#)]
218. Choi, K.S.; Choi, S.H.; Jeong, B. Prediction of IDH genotype in gliomas with dynamic susceptibility contrast perfusion MR imaging using an explainable recurrent neural network. *Neuro Oncol.* **2019**, *21*, 1197–1209. [[CrossRef](#)]
219. Bisdas, S.; Sanverdi, E.; Sudre, C.; Roettger, D.; Brandner, S.; Katsaros, V. The role of dynamic susceptibility contrast perfusion-weighted MRI in the estimation of IDH mutation in gliomas. *J. Clin. Oncol.* **2018**, *36*, 12063. [[CrossRef](#)]
220. Priya, S.; Liu, Y.; Ward, C.; Le, N.H.; Soni, N.; Pillenahalli Maheshwarappa, R.; Monga, V.; Zhang, H.; Sonka, M.; Bathla, G. Machine learning based differentiation of glioblastoma from brain metastasis using MRI derived radiomics. *Sci. Rep.* **2021**, *11*, 10478. [[CrossRef](#)]

221. Jeong, J.; Wang, L.; Ji, B.; Lei, Y.; Ali, A.; Liu, T.; Curran, W.J.; Mao, H.; Yang, X. Machine-learning based classification of glioblastoma using delta-radiomic features derived from dynamic susceptibility contrast enhanced magnetic resonance images. *Quant. Imaging Med. Surg.* **2019**, *9*, 1201213. [[CrossRef](#)]
222. Kim, J.Y.; Park, J.E.; Jo, Y.; Shim, W.H.; Nam, S.J.; Kim, J.H.; Yoo, R.-E.; Choi, S.H.; Kim, H.S. Incorporating diffusion- and perfusion-weighted MRI into a radiomics model improves diagnostic performance for pseudoprogression in glioblastoma patients. *Neuro Oncol.* **2019**, *21*, 404–414. [[CrossRef](#)]
223. Elshafeey, N.; Kotrotsou, A.; Hassan, A.; Elshafei, N.; Hassan, I.; Ahmed, S.; Abrol, S.; Agarwal, A.; El Salek, K.; Bergamaschi, S.; et al. Multicenter study demonstrates radiomic features derived from magnetic resonance perfusion images identify pseudoprogression in glioblastoma. *Nat. Commun.* **2019**, *10*, 3170. [[CrossRef](#)] [[PubMed](#)]
224. Siakallis, L.; Sudre, C.H.; Mulholland, P.; Fersht, N.; Rees, J.; Topff, L.; Thust, S.; Jager, R.; Cardoso, M.J.; Panovska-Griffiths, J.; et al. Longitudinal structural and perfusion MRI enhanced by machine learning outperforms standalone modalities and radiological expertise in high-grade glioma surveillance. *Neuroradiology* **2021**, *63*, 2047–2056. [[CrossRef](#)] [[PubMed](#)]
225. Park, J.E.; Kim, H.S.; Jo, Y.; Yoo, R.-E.; Choi, S.H.; Nam, S.J.; Kim, J.H. Radiomics prognostication model in glioblastoma using diffusion- and perfusion-weighted MRI. *Sci. Rep.* **2020**, *10*, 4250. [[CrossRef](#)] [[PubMed](#)]
226. Shim, K.Y.; Chung, S.W.; Jeong, J.H.; Hwang, I.; Park, C.-K.; Kim, T.M.; Park, S.-H.; Won, J.K.; Lee, J.H.; Lee, S.-T.; et al. Radiomics-based neural network predicts recurrence patterns in glioblastoma using dynamic susceptibility contrast-enhanced MRI. *Sci. Rep.* **2021**, *11*, 9974. [[CrossRef](#)]